https://www.youtube.com/watch?v=q5K_w9Tbhoc

CRACKING THE CONCH CONUNDRUM: REVERSE ENGINEERING OF THE SHELLS OF MOLLUSKS

Roberto Ballarini
University of Houston

Collaborators:

Arthur Heuer
Arnold Caplan
Shekar Kamat
Hannes Kessler
Maissarath Nassirou
Liisa Kuhn
Mark Spearing
Vince Laria

City University of Hong Kong
January 7, 2019

What is an ideal composite?

It should be comprised of readily available and inexpensive materials.

It should be strong, tough and light.

It should be capable of self-healing.

It should not require prohibitive manufacturing processes.

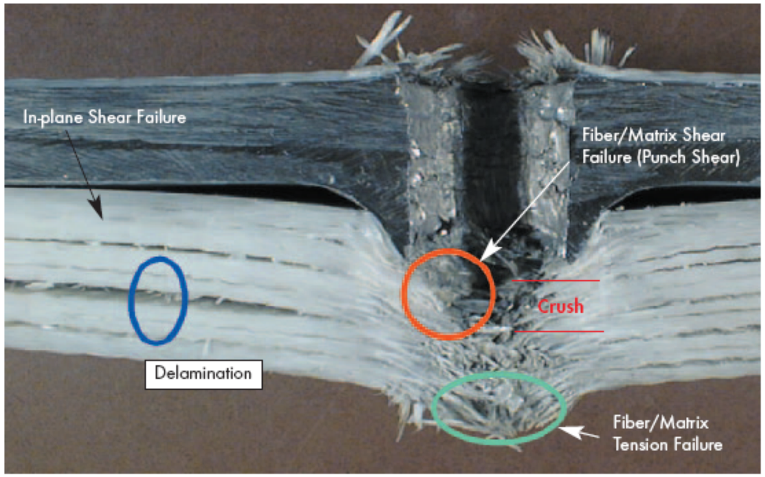

Figure 6. Damage Mechanisms Observed During the Impact and Penetration of a Composite.

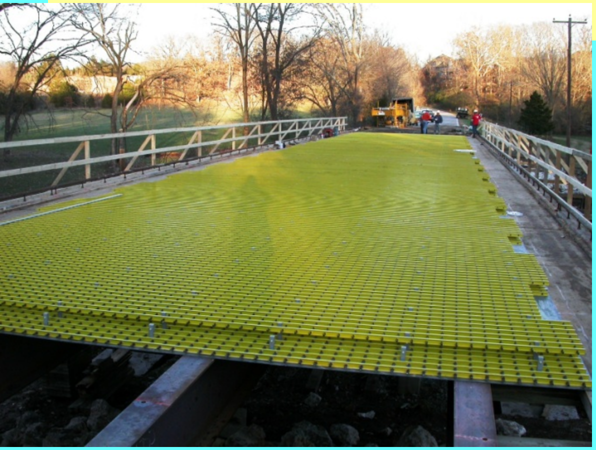

Let's turn to *Nature* for inspiration.

STROMBUS GIGAS: WHY IS IT SO TOUGH?

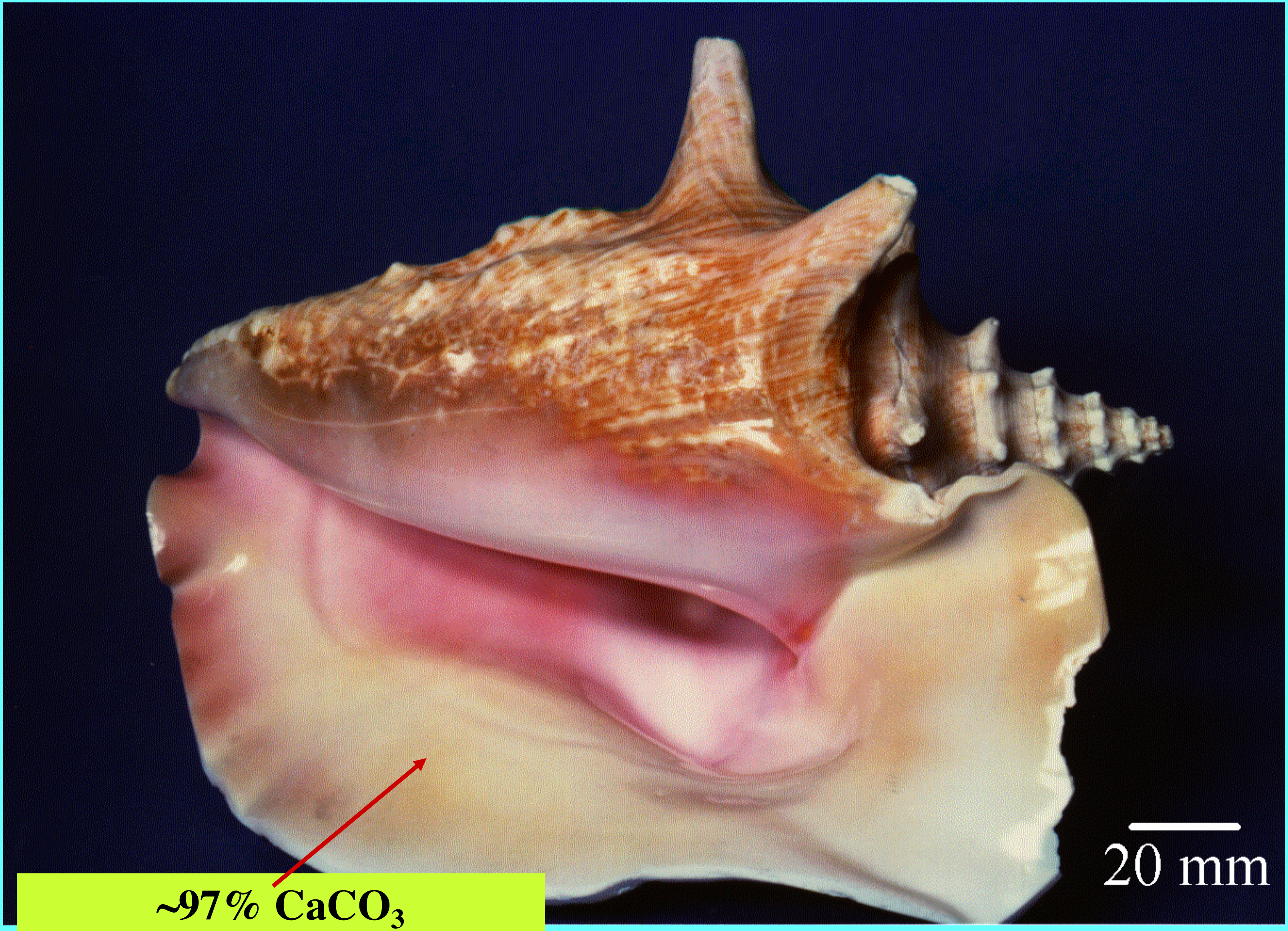

~97% $CaCO_3$
~3% protein binder

Aragonite is brittle (flaw-sensitive), but available.

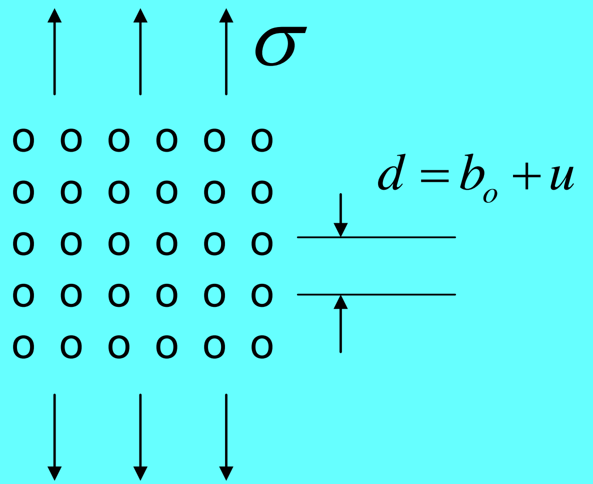

$$\frac{\sigma_f}{\sigma_{th}} = \frac{1}{\sqrt{\pi}} \frac{m}{(n/m)^{n/(m-n)}\sqrt{(n-1)(m-1)}} \sqrt{\frac{b_o}{a}}$$

perfect lattice

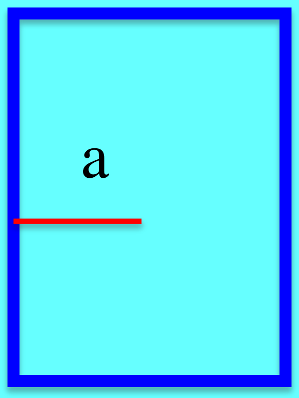

cracked lattice

$b_o \sim 10^{-10}$m

if $a \sim 10^{-4}$m

Then ratio is 1/1000!!

http://www.gereports.com/post/110549411475/ceramic-matrix-composites-allow-ge-jet-engines-to/

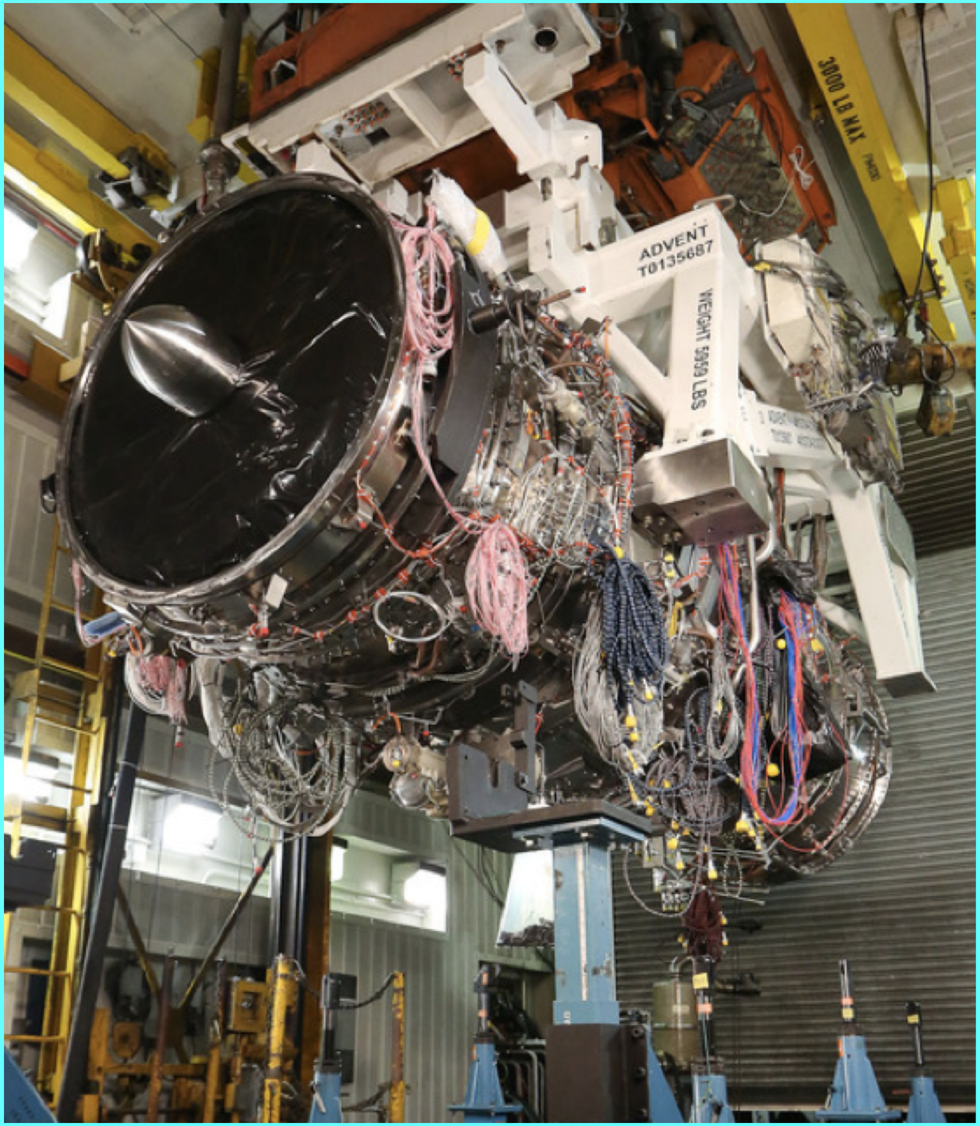

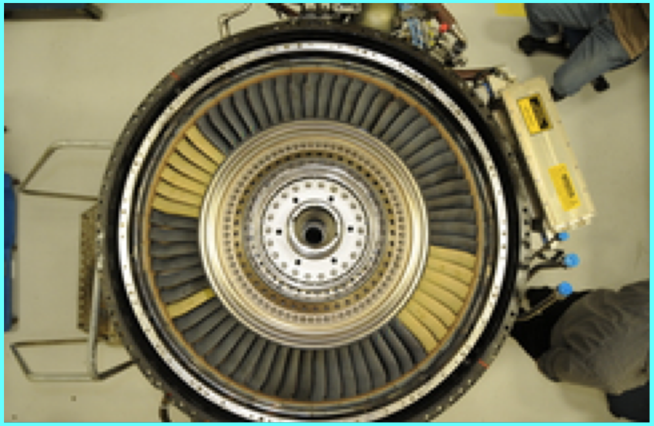

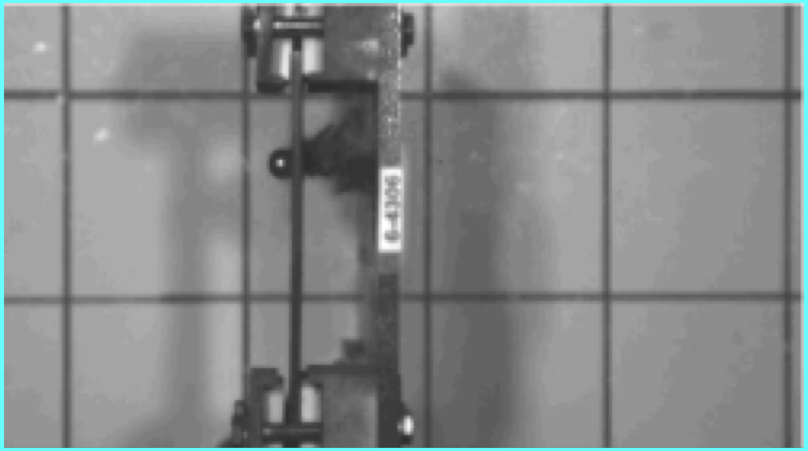

GE CMC Engine

PREDATORS

Spiny Lobster

Southern Stingray

Loggerhead Turtle

Blue Crab

Octopus

Porcupine Fish


© SeaPics.com

MATERIAL SELECTION CHARTS AND MATERIAL INDICES

M. Ashby, *Materials Selection in Mechanical Design*: Pergamon, 1992

Design	Tie in tension	Beam in Flexure	Plate in Flexure
Strength to weight	σ_f / ρ	$\sigma_f^{2/3} / \rho$	$\sigma_f^{1/2} / \rho$
Stiffness to weight	E / ρ	$E^{1/2} / \rho$	$E^{1/3} / \rho$
Large recoverable deformation	σ_f / E	σ_f / E	σ_f / E
Strain energy per volume	σ_f^2 / E	σ_f^2 / E	σ_f^2 / E

Material	E GPa	ρ Mg/m^3	E/ρ GPa/Mg/m^3	$E^{1/2}/\rho$ GPa$^{1/2}$/Mg/m^3	$E^{1/3}/\rho$ GPa$^{1/2}$/Mg/m^3
Palm	**3.5**	**0.15**	**23**	**12.5**	**(10.1)**
Mild steel	**210**	**7.9**	**27**	**1.8**	**(0.8)**
Balsa wood (LD)	**2.0**	**0.1**	**20**	**14.1**	**(12.6)**

Material	σ_f MPa	ρ Mg/m^3	σ_f / ρ $MPa/Mg/m^3$	$\sigma_f^{2/3} / \rho$ $MPa^{2/3}/Mg/m^3$	$\sigma_f^{1/2} / \rho$ $MPa^{1/2}/Mg/m^3$
Single silk fibre	2000	1.3	1500	120	(35)
Single carbon fibre	2200	2.0	1100	85	(24)
Mild steel	400	7.9	51	6.9	2.5
Balsa wood (LD)	16	0.1	160	64	(40.0)

CRACK TIP PARAMETERS

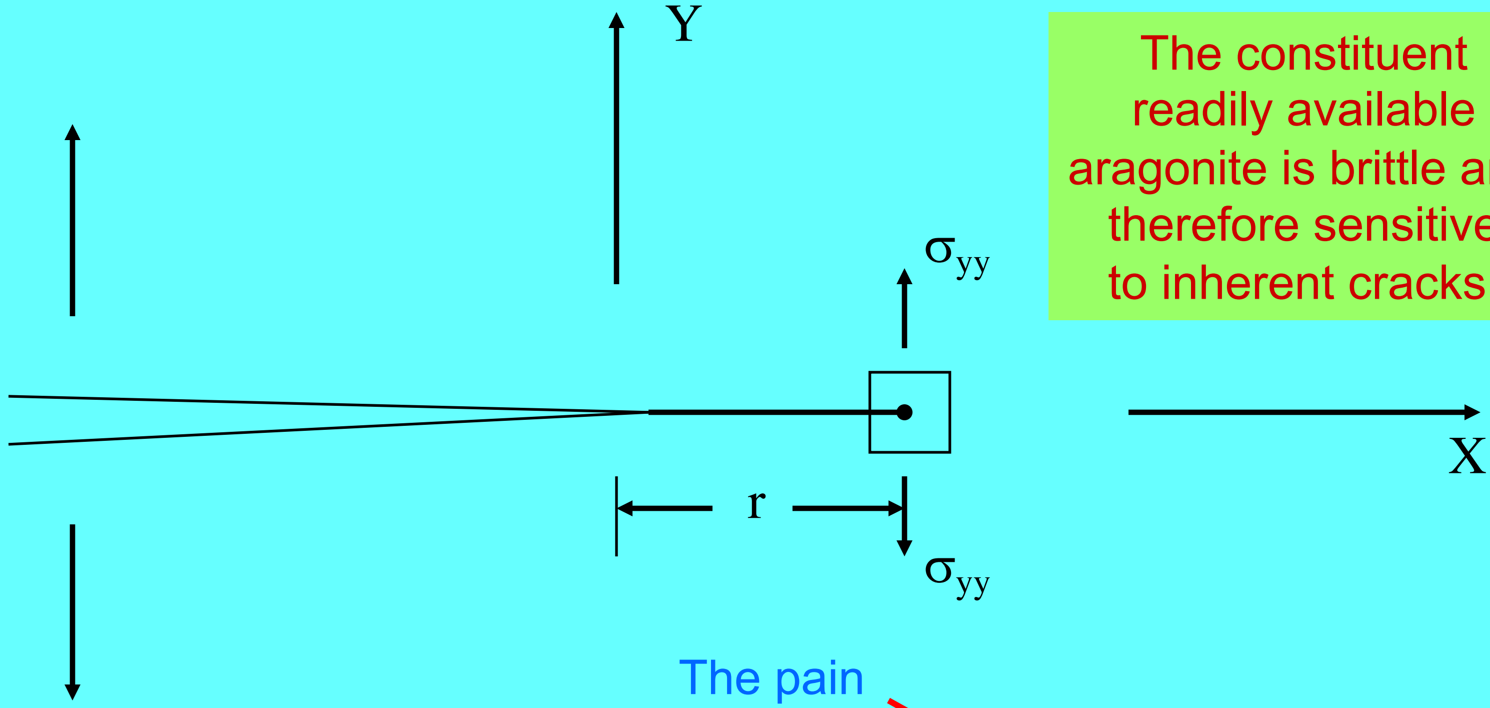

The constituent readily available aragonite is brittle and therefore sensitive to inherent cracks.

$$\sigma_{yy} \approx \sqrt{\frac{EJ}{r}}$$

The pain felt by the material.

J_c , a material property, is all the pain it can take before the crack grows.

Material	E GPa	$(EJ_c)^{1/2}$ MPa-m$^{1/2}$	J_c kJ/m^2	$(J_c/E)^{1/2}$ mm$^{1/2}$
Antler	10	7.1	5.0	0.7
Mollusc shell	60	9.5	1.5	0.4
Mild steel	210	90	40	0.4
Skin	0.01	0.4	15.0	38.7

If a material contains an inherent crack

Load carrying capacity ~ $(EJ_c)^{1/2}$

Impact energy absorption ~ J_c

Displacement capacity ~ $(J_c/E)^{1/2}$

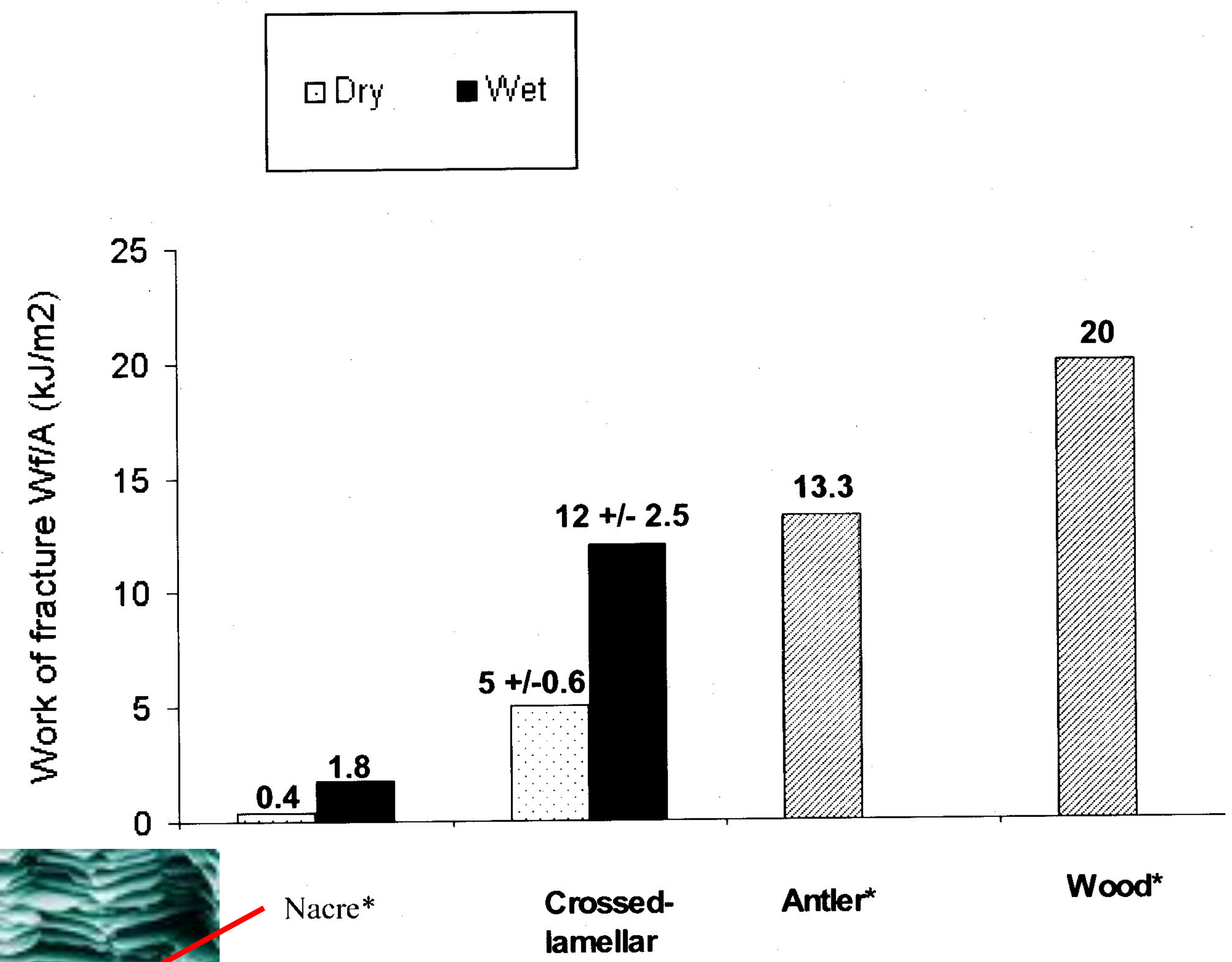

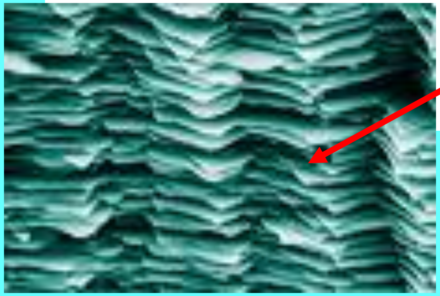

A.A.Jackson, J.F.V. Vincent and R.M. Turner (1990)
J. Mat. Sci. 25, p3137

Basilica di Santa Maria del Fiore (Duomo)
Brunelleschi
Competition to design the dome started in 1419; the work was completed in 1436

Achievements

•~140 ft span (wider than Pantheon).
•Base of dome ~180 ft above ground (higher than in any Gothic cathedral).
•Too high and too large for any kind of centering.
•For aesthetics, built without any external buttressing.
•The cathedral design model required an octagonal dome profile with visible external ribs.

Two factors played a crucial role in the dome's construction:

•Efficient worksite organization (construction management).
•Machines capable of heavy lifting to great heights.

**Brunelleschi left no records of his machines.
Fortunately a number of 15th century engineers,
including the young Leonardo, recorded them in their drawings.**

Museo del Duomo

Brunelleschi was inspired by the Pantheon
But he did not use concrete, nor scaffolding

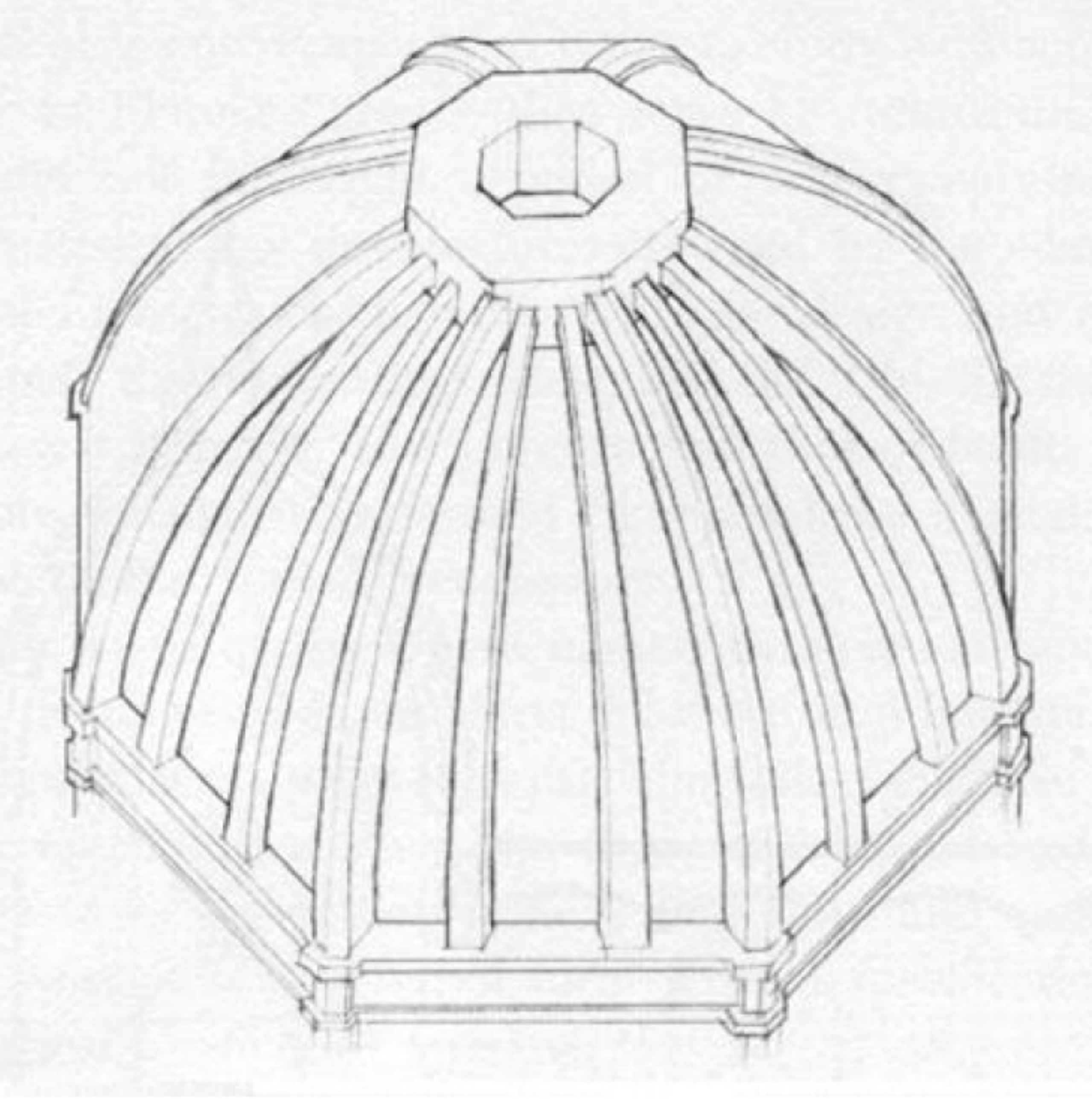

The skeleton ribs of the dome.

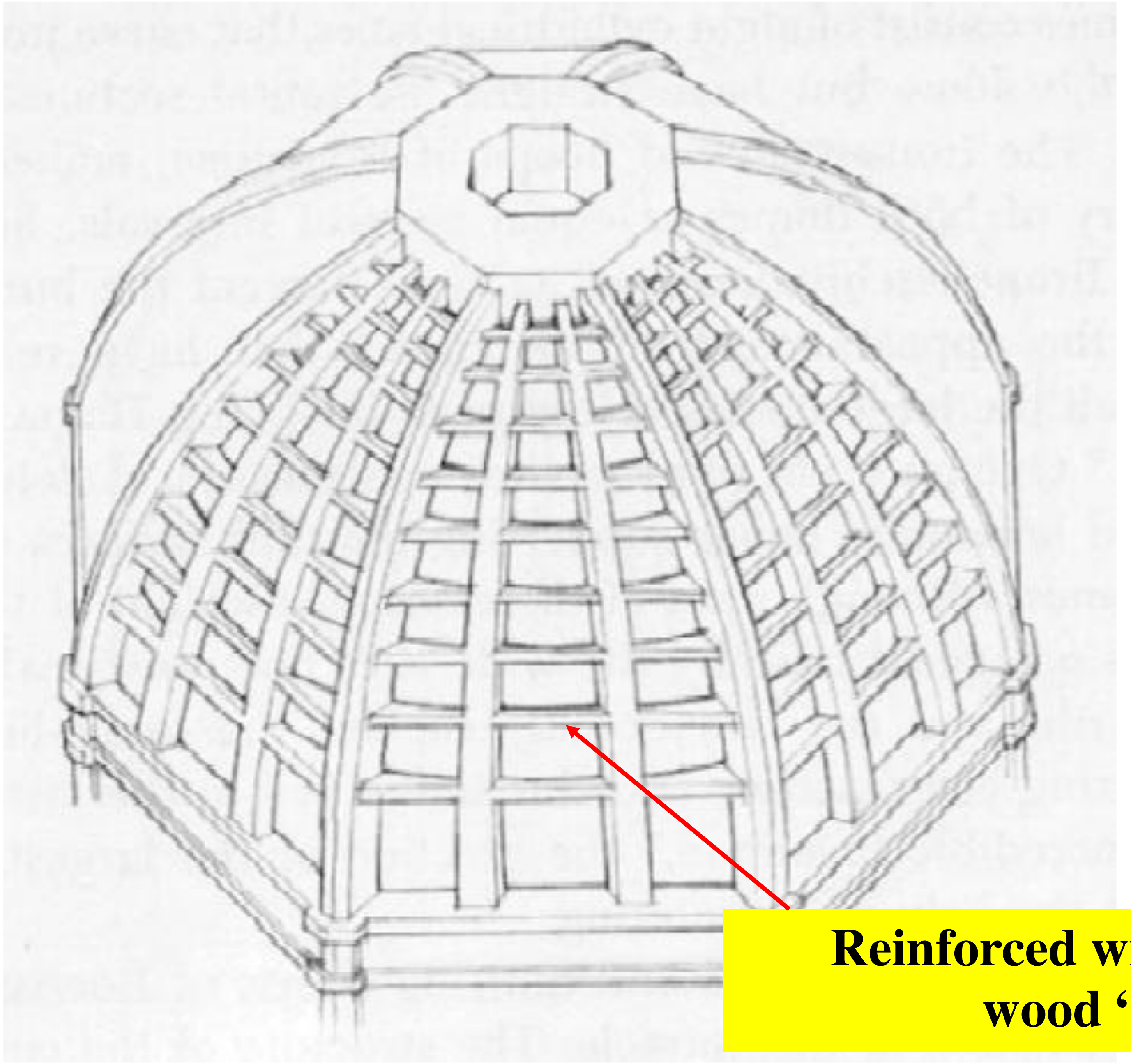

The nine horizontal circles that tie the ribs together.

Reinforced with stone a
wood "rods"

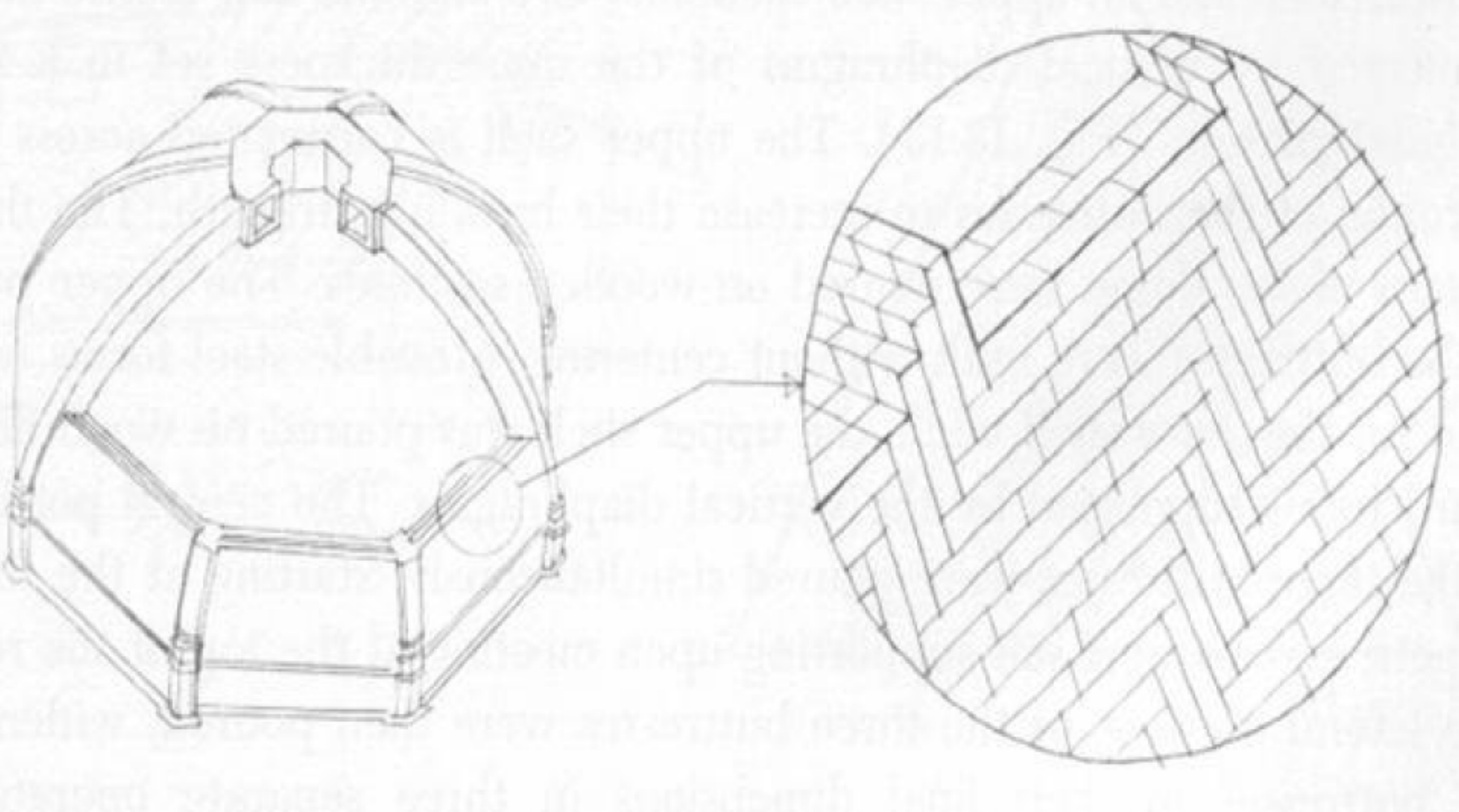

The brick masonry was laid in this herringbone pattern.

BRUNELLESCHI's DOME IN FLORENCE: monitoring system

View of a 70 cm displacement transducer

DISPLACEMENT TRANSDUCERS

- Total number: 72
- Inductive transducers
- Accuracy: ±0.02 mm
- Tangential and normal displacements

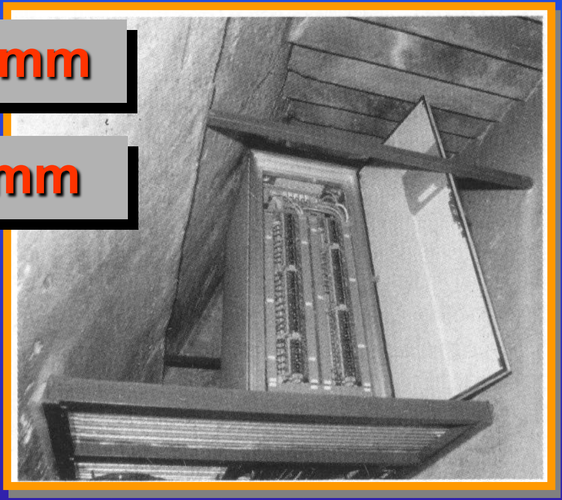

View of a peripheral device

THERMOMETERS

- Total number: 60
- Resistive transducers
- Accuracy: ±0.05 °C
- Placed externally, in masonry and in the interspace between the two domes

BRUNELLESCHI's DOME IN FLORENCE: monitoring system

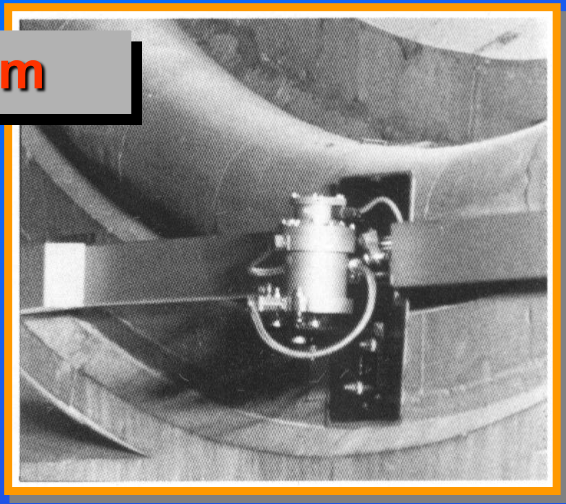

View of a levelling instrument

LEVELLING INSTRUMENTS

- Total number: 8
- Hydraulic oil circuit

View of a telecoordinometer

TELECOORDINOMETERS

- Total number: 8
- Photoelectric cells
- Displacements are read at three levels in X and Y directions

Correlation among temperatures

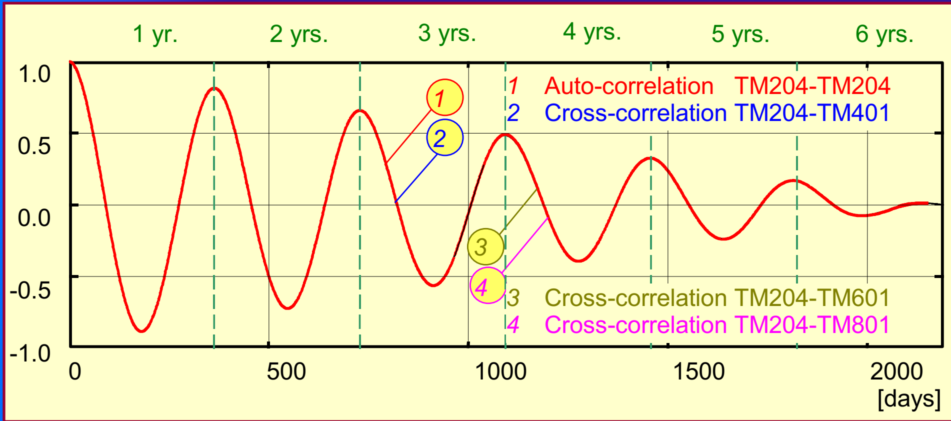

PARALLEL DIRECTION

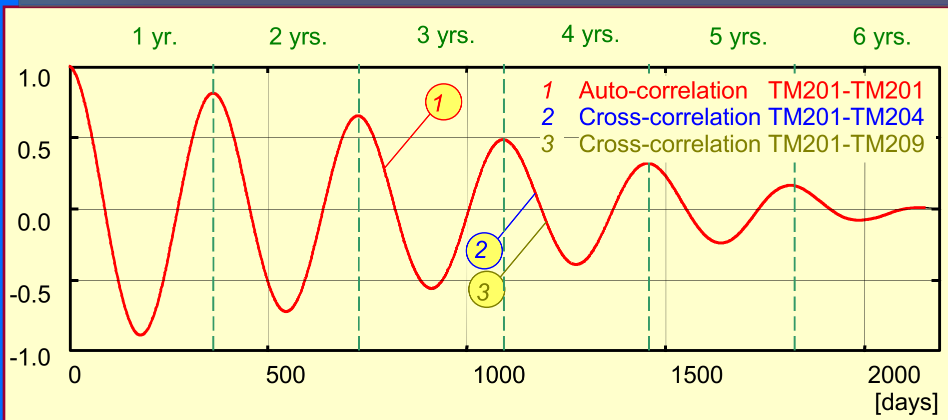

MERIDIAN DIRECTION

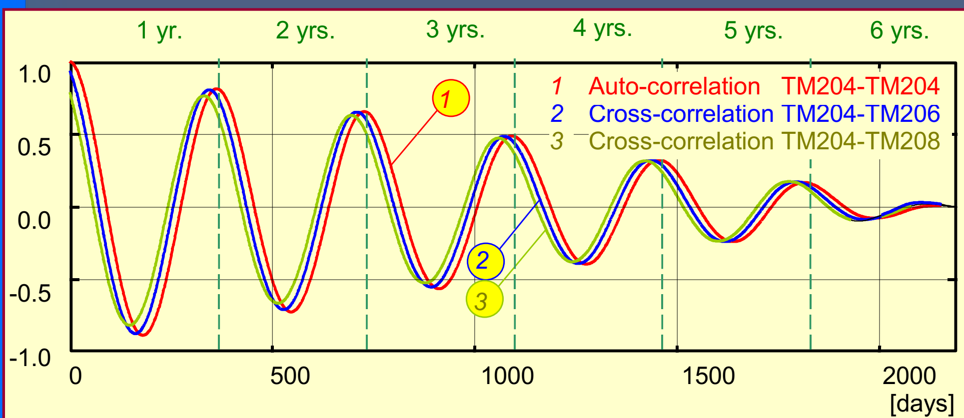

RADIAL DIRECTION

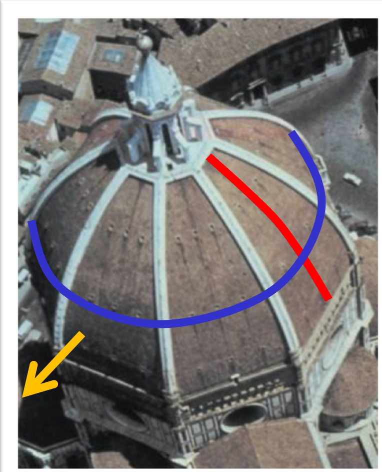

BRUNELLESCHI's DOME IN FLORENCE: the numerical model

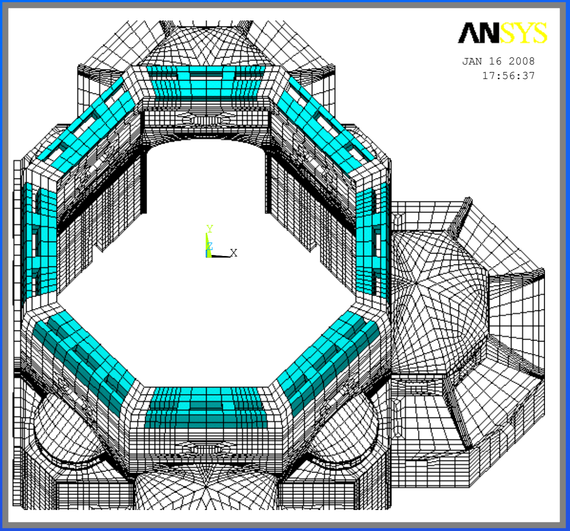

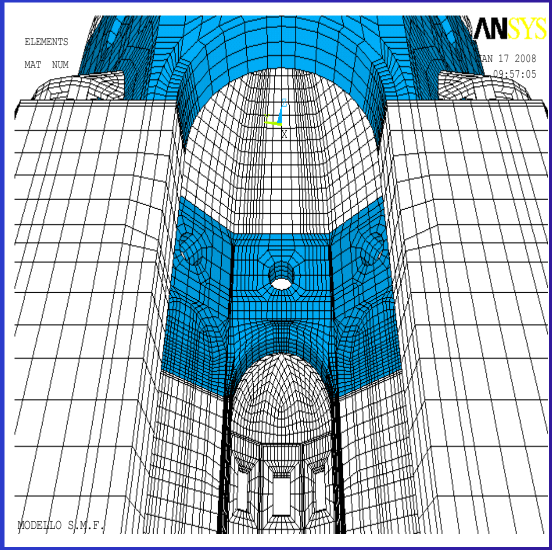

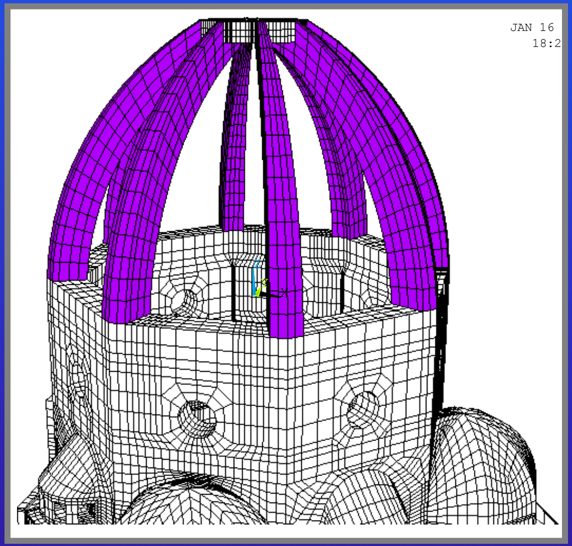

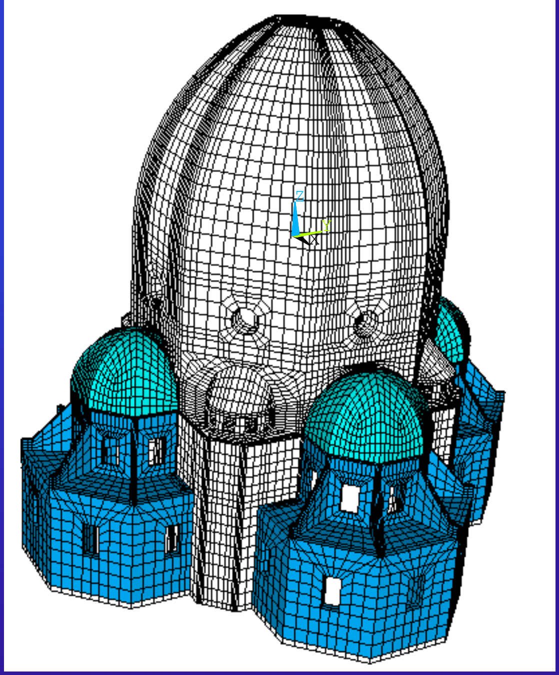

CRACKS IDENTIFICATION

BRUNELLESCHI's DOME IN FLORENCE: the numerical model

BRUNELLESCHI's DOME IN FLORENCE: the numerical model

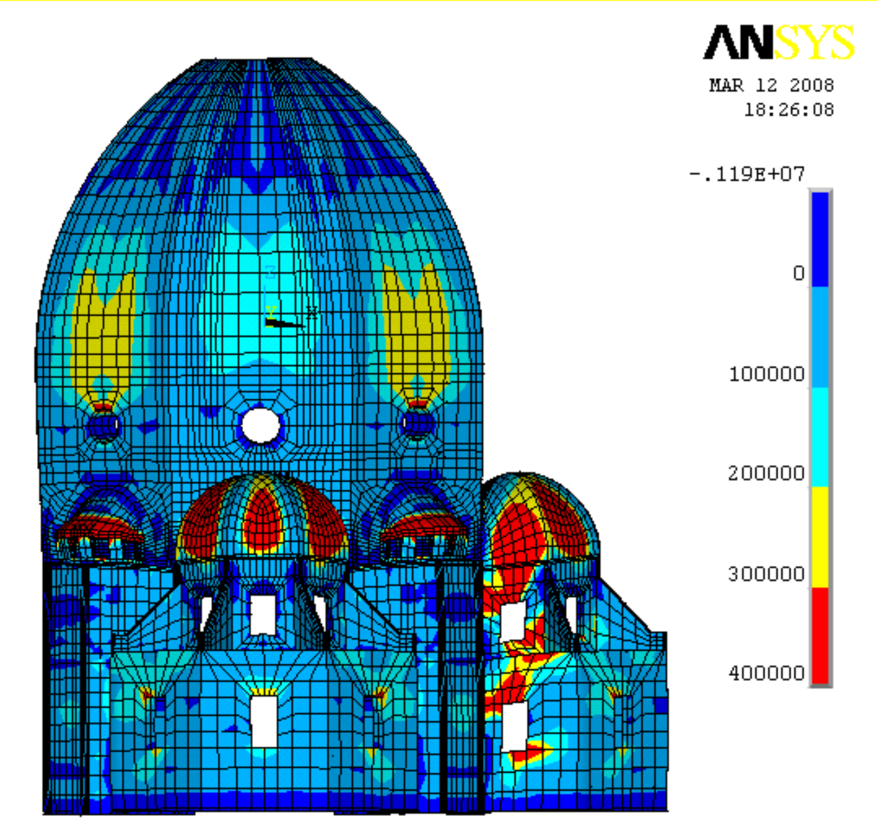

Dead load (own weight): single step

(unrealistic tensile stresses distribution)

- geometric non linear step-by-step restart analyses to reproduce the constructive phases

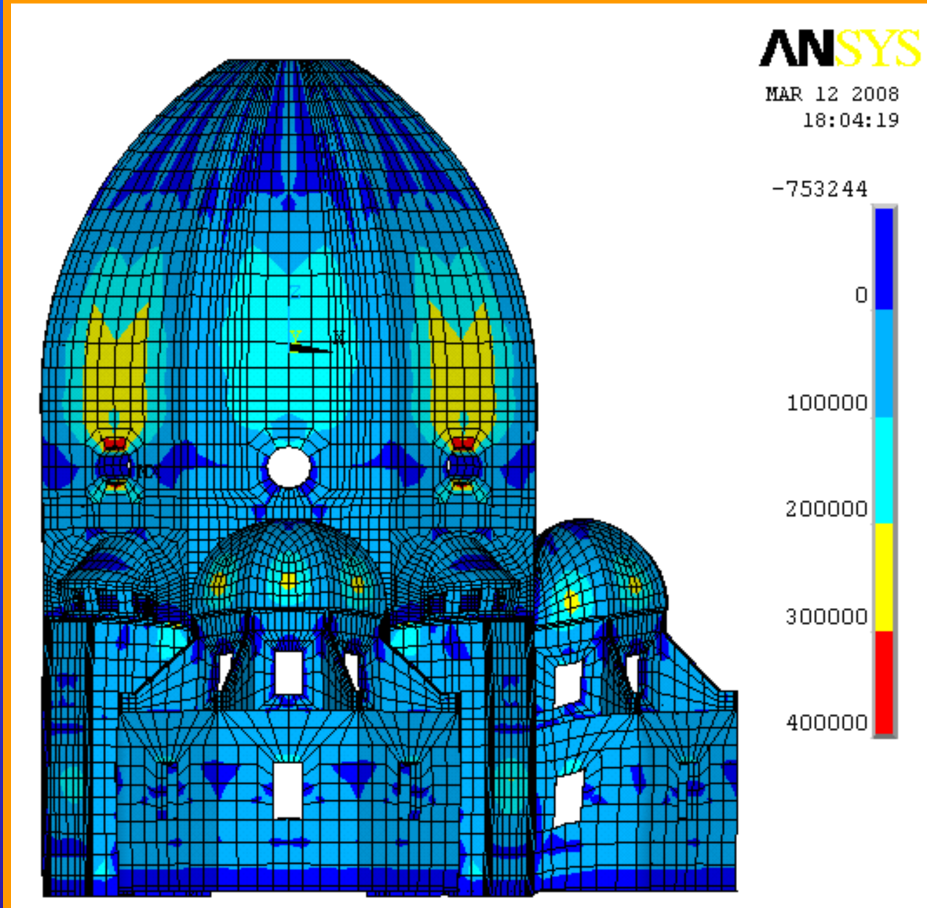

BRUNELLESCHI's DOME IN FLORENCE: seismic vulnerability assessment

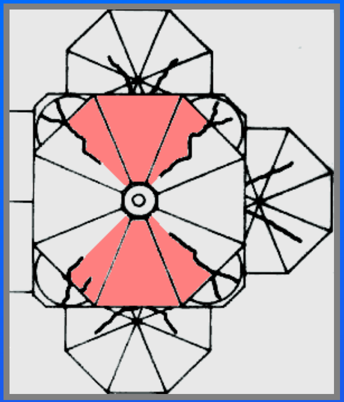

LOAD DIRECTION

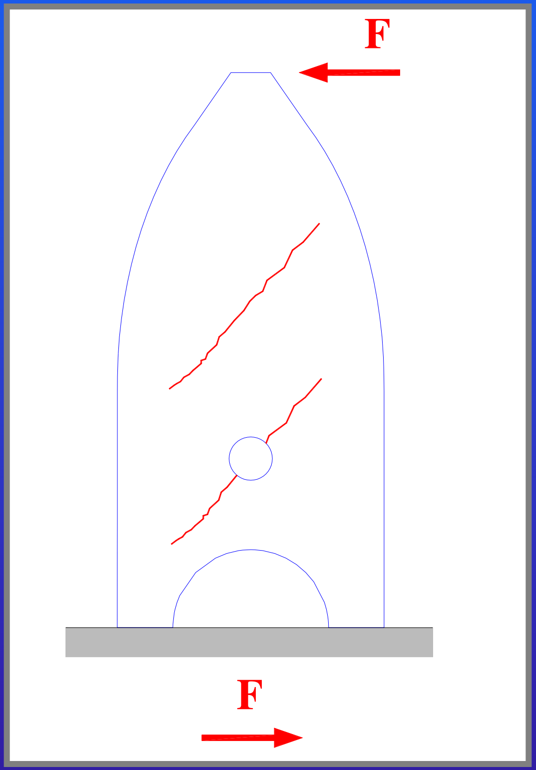

- PRINCIPAL TENSILE STRESS: 45°
- OPENING OF CRACK

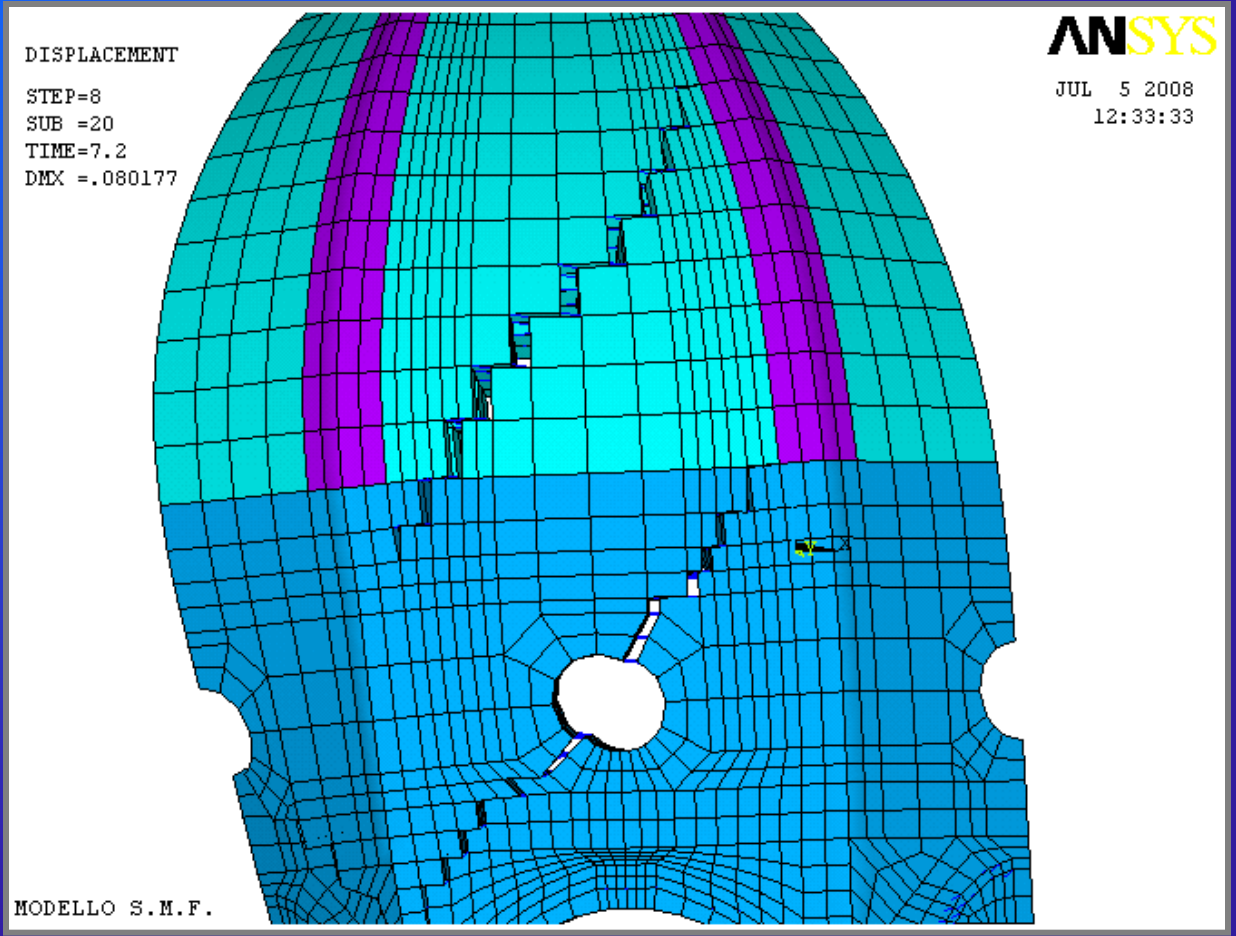

“Classical” solution

BRUNELLESCHI’s DOME IN FLORENCE

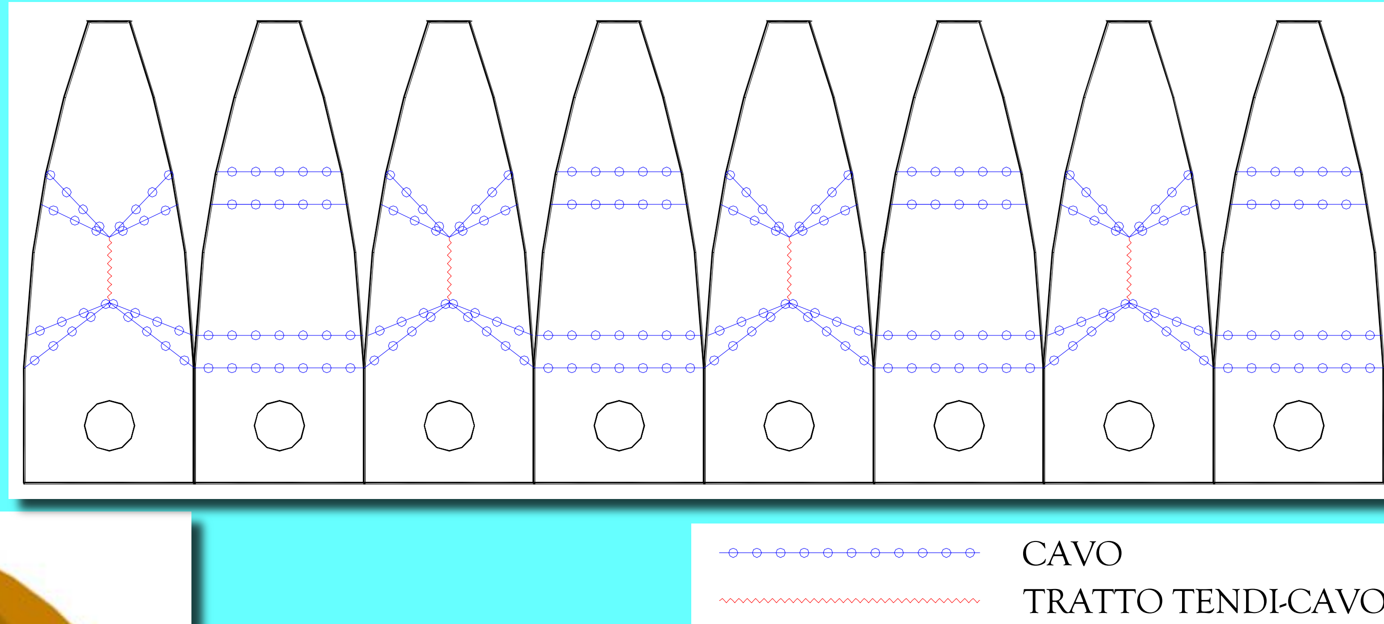

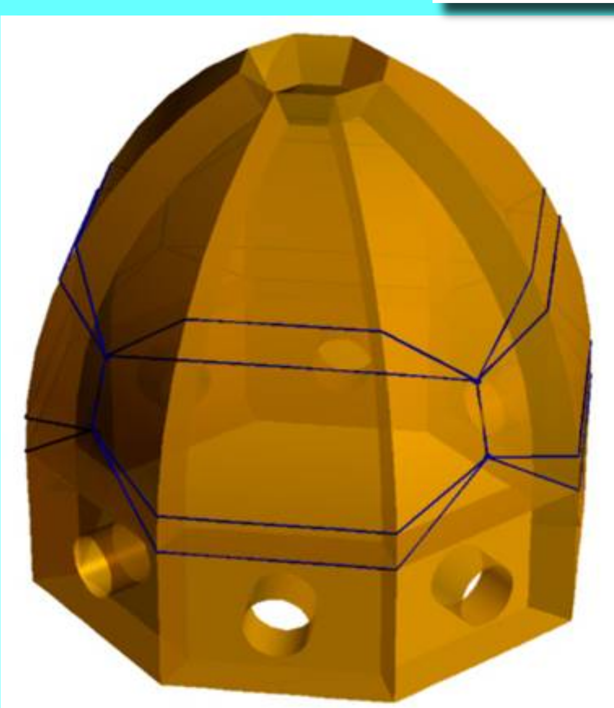

Advantages:

- no cables overlapping
- easier post-tensioning

Disadvantages:

- less efficient solution
- irregular points at some positions

An example of synergy between disciplines

REFERENCES

"Secrets dans la Coquille," ***Pour La Science*****, 2008.**

"Secrets in the Shell," ***American Scientist*****, 2007.**

"Fracture Mechanisms of the *Strombus gigas* Conch Shell: II Micromechanics Analyses of Multiple Cracking and Large Scale Crack Bridging," ***Acta Materialia*****, 2004.**

"Structural Basis for the Fracture Toughness of the Shell of the Conch Strombus Gigas," ***Nature*****, 2000.**

"A Biomimetic Example of Brittle Toughening: Steady State Multiple Cracking," ***Computational Materials Science*****, 1996.**

Microstructure

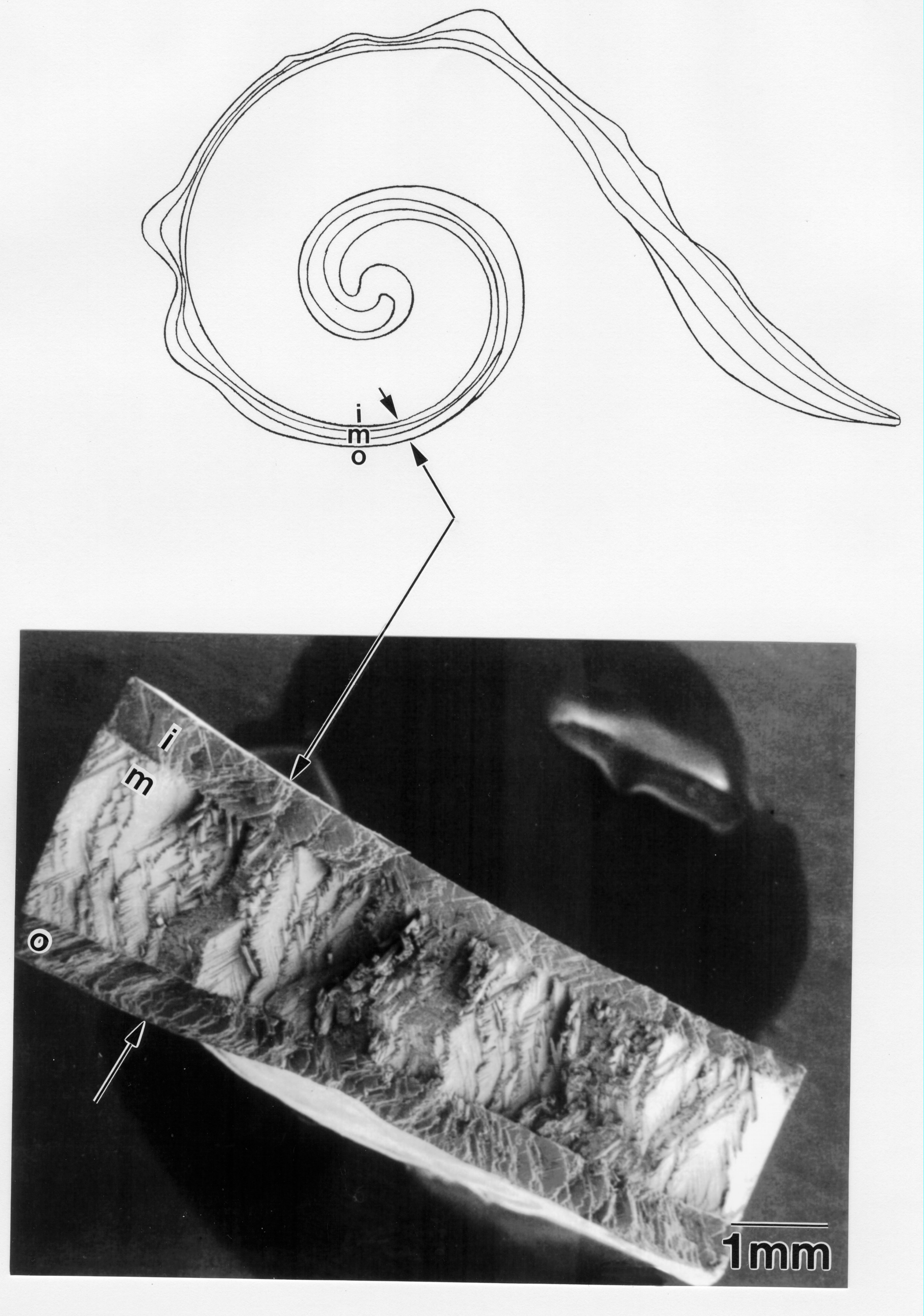

CROSSED-LAMELLAR MICROARCHITECTURE

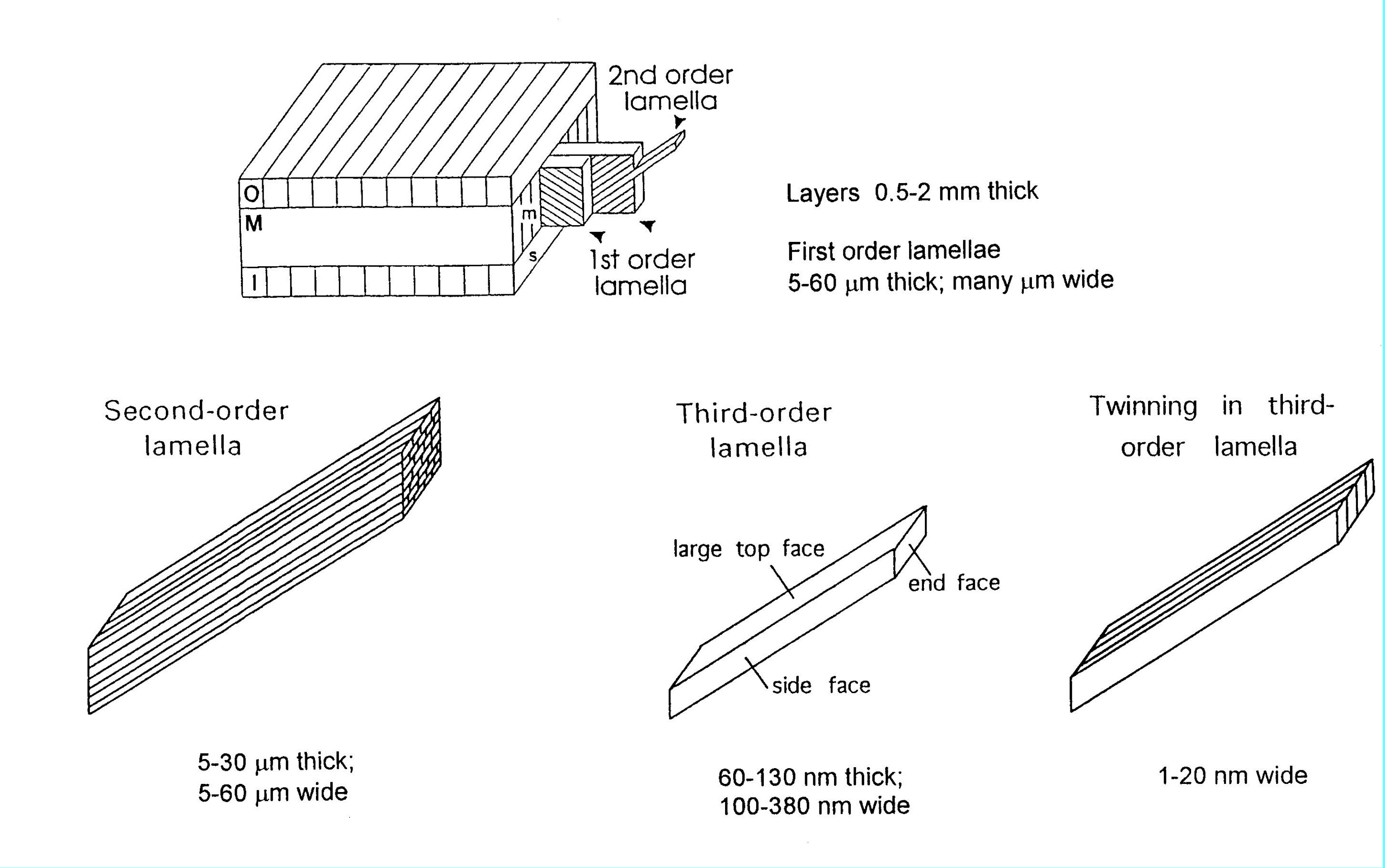

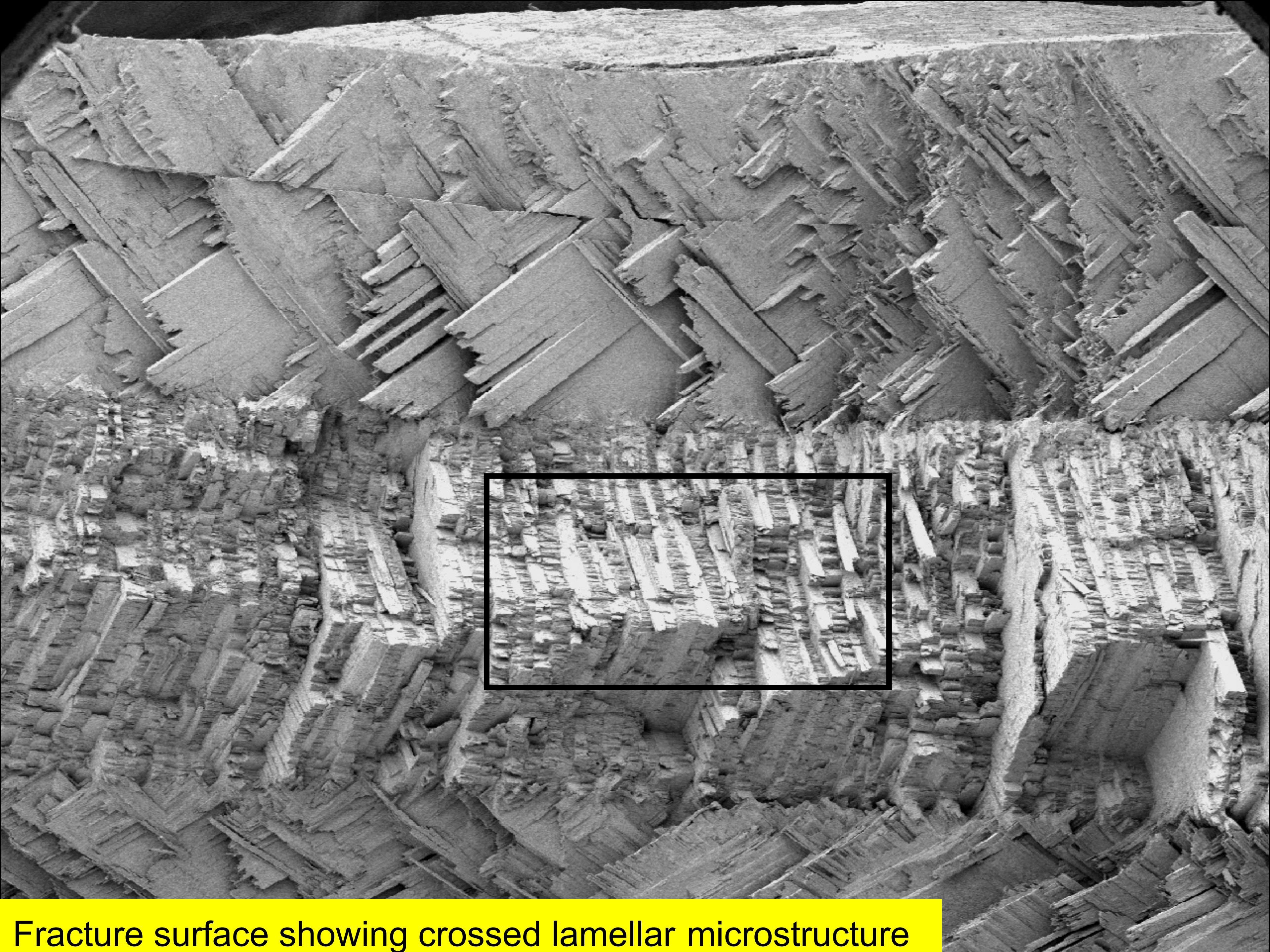

Fracture surface showing crossed lamellar microstructure

Higher Magnification SEM Images

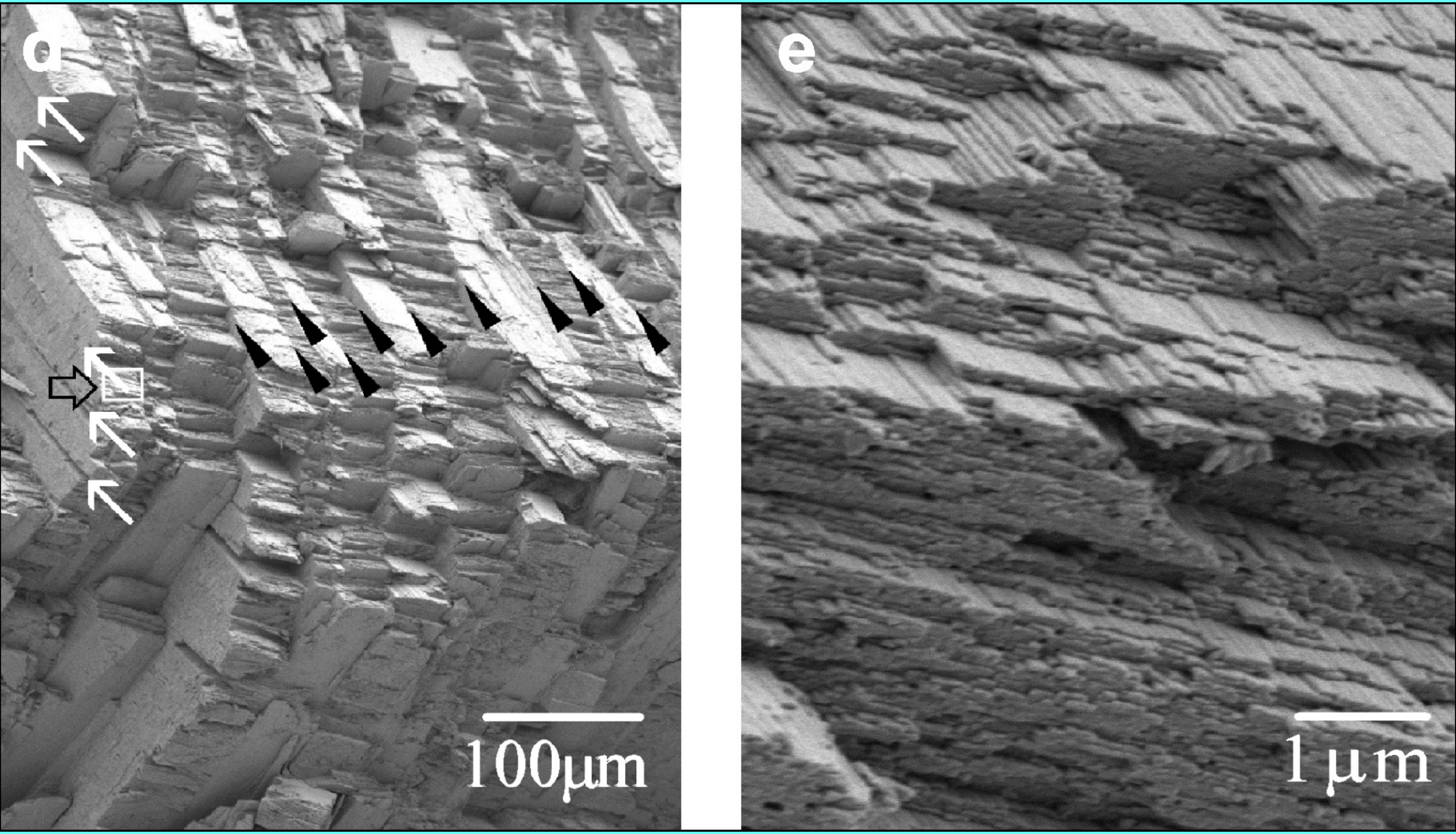

TEM MICROGRAPH OF THE INTERFACE BETWEEN SINGLE CRYSTALS OF ARAGONITE

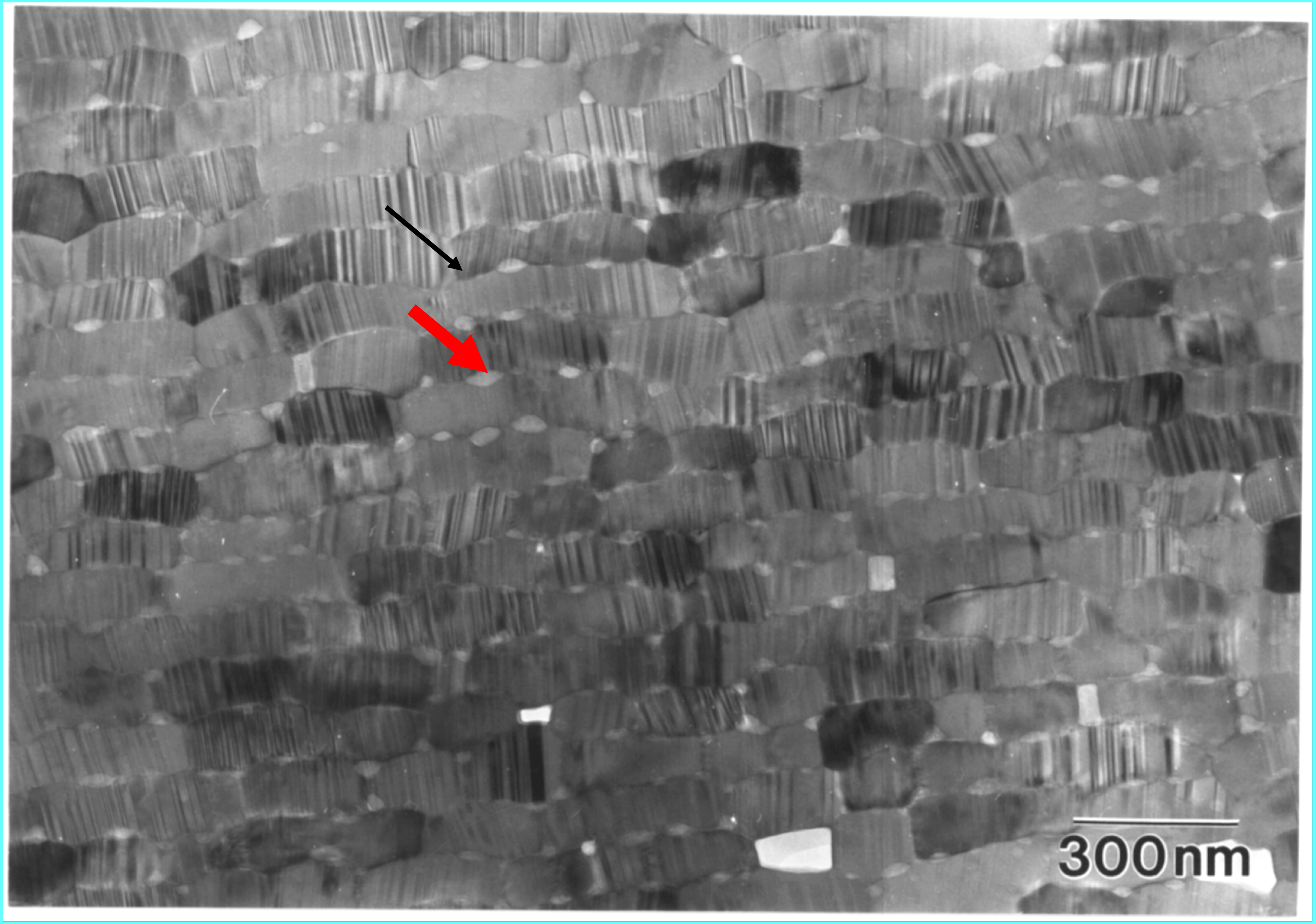

REVERSE ENGINEERING

Microstructure

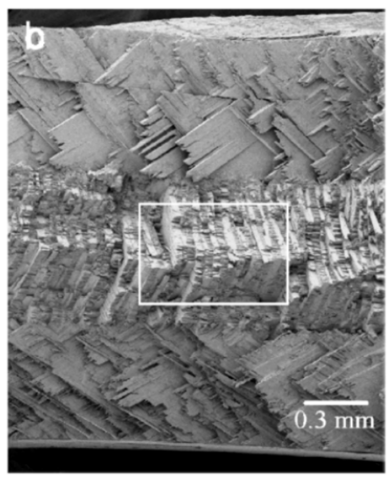

Dominant fracture mechanisms

Tunnel cracking

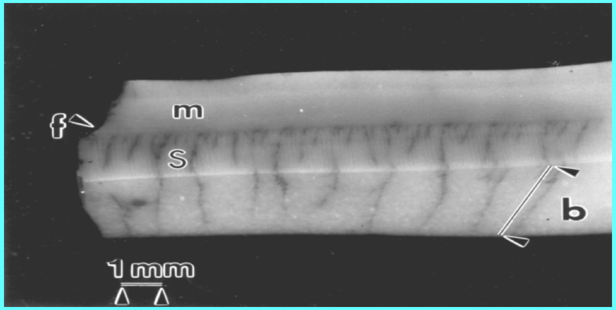

Crack bridging

Modeling

Steady-state tunneling

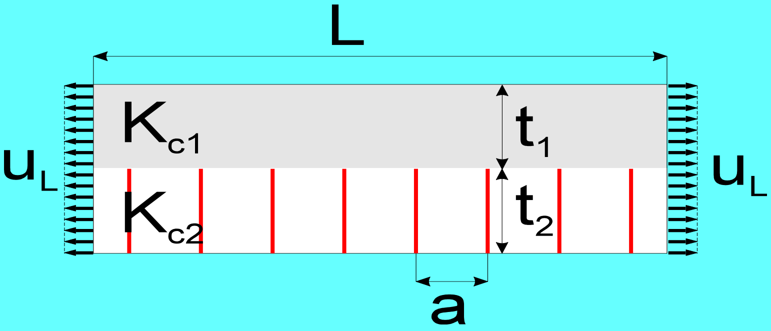

Crack bridging

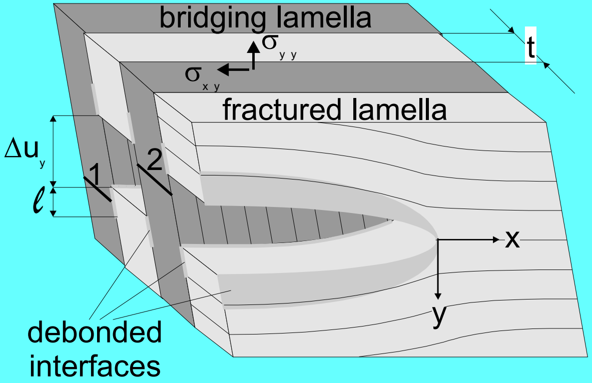

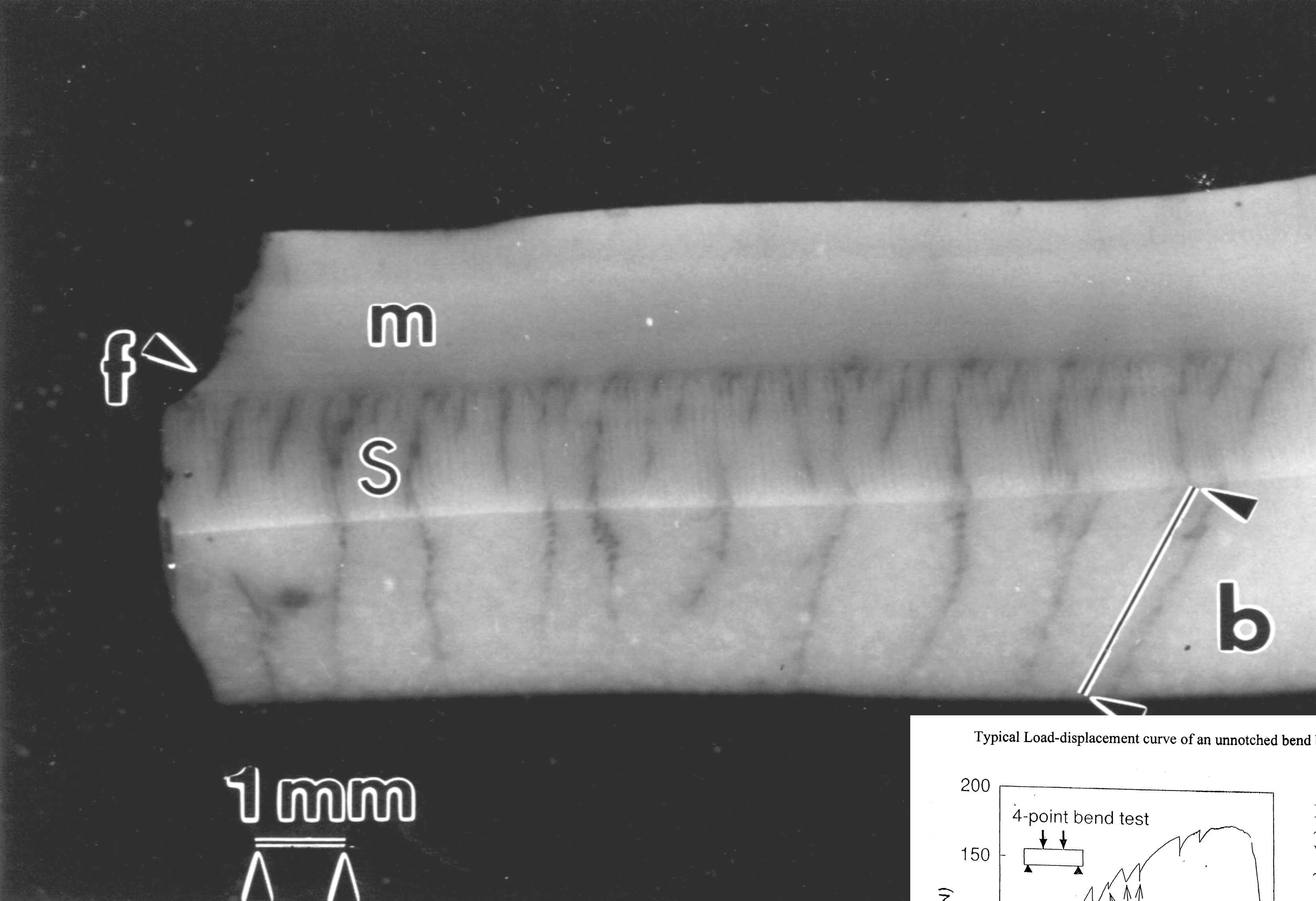

Typical Load-displacement curve of an unnotched bend bar at Room Temperature.

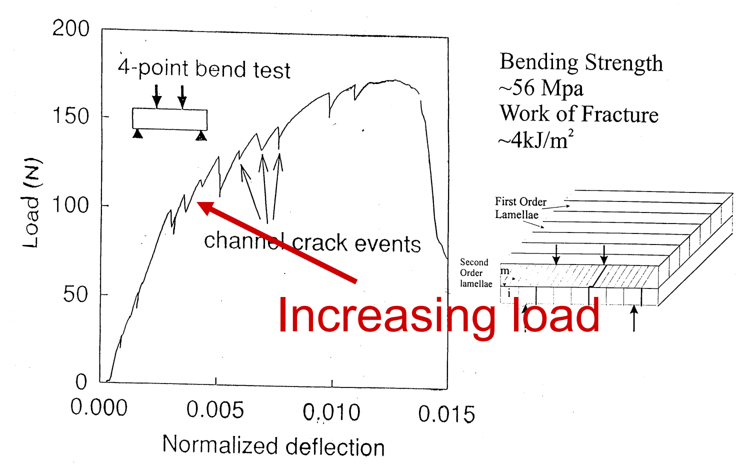

NOTCHED SAMPLE RESULTS

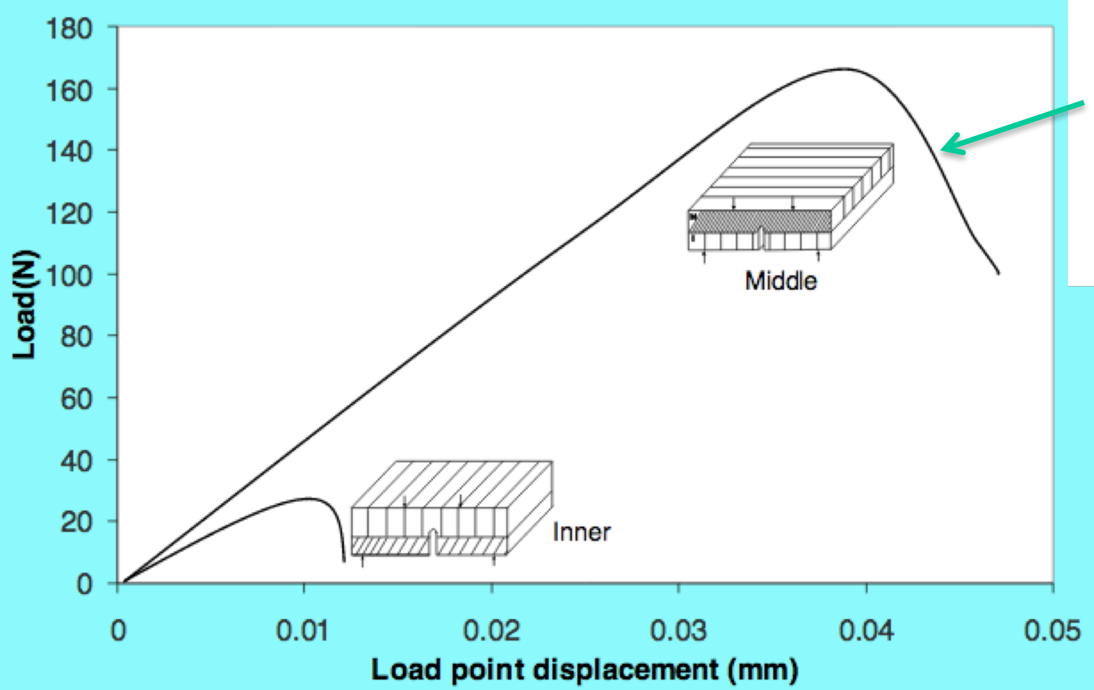

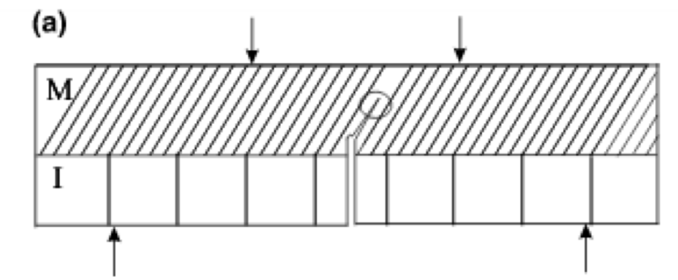

Nominal fracture toughness

inner layer: 0.46 ± 0.15 $MPa\ m^{1/2}$ ***(Use 0.6 in calculations)***

middle layer: 2.26 ± 0.77 $MPa\ m^{1/2}$

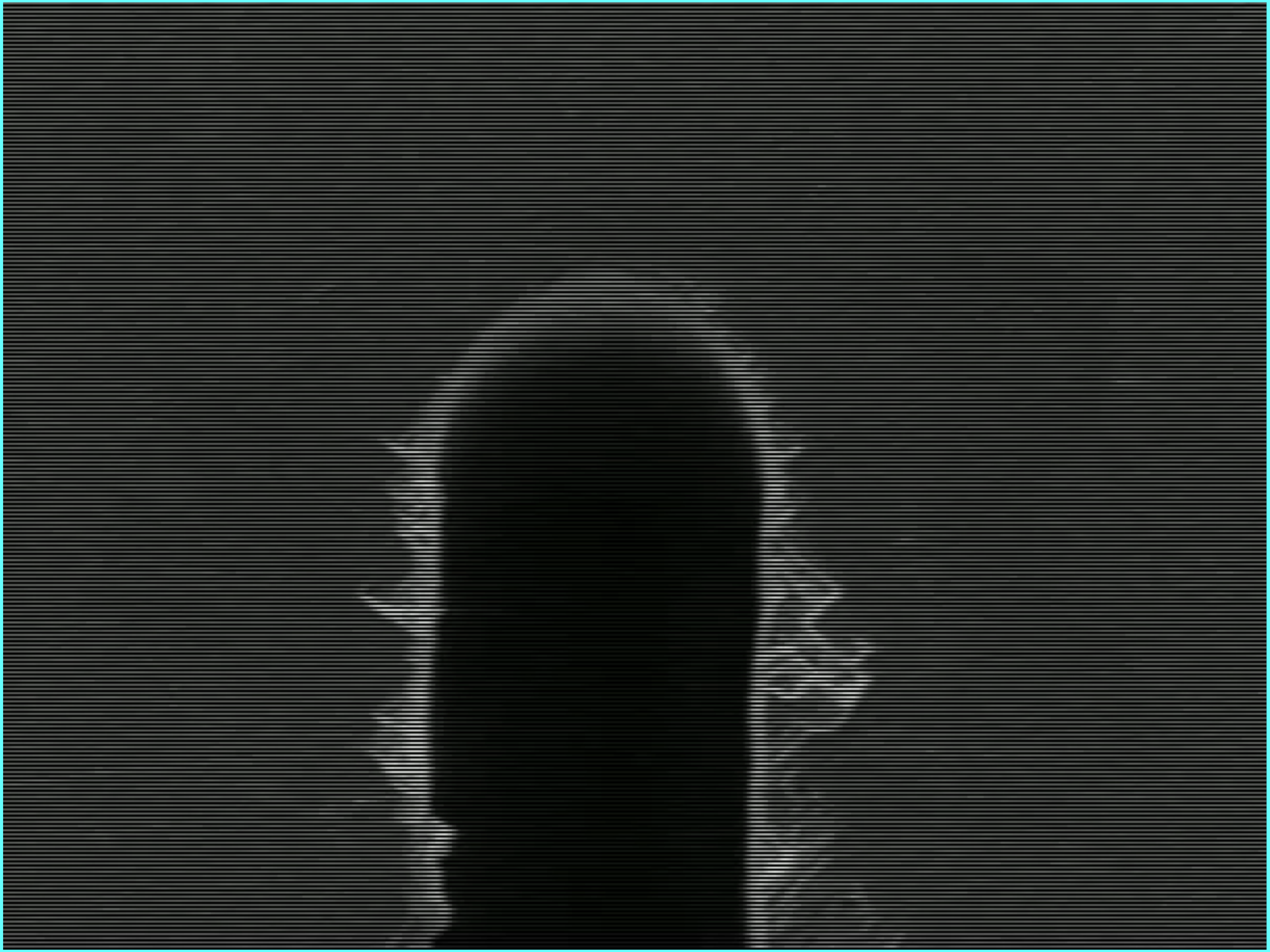

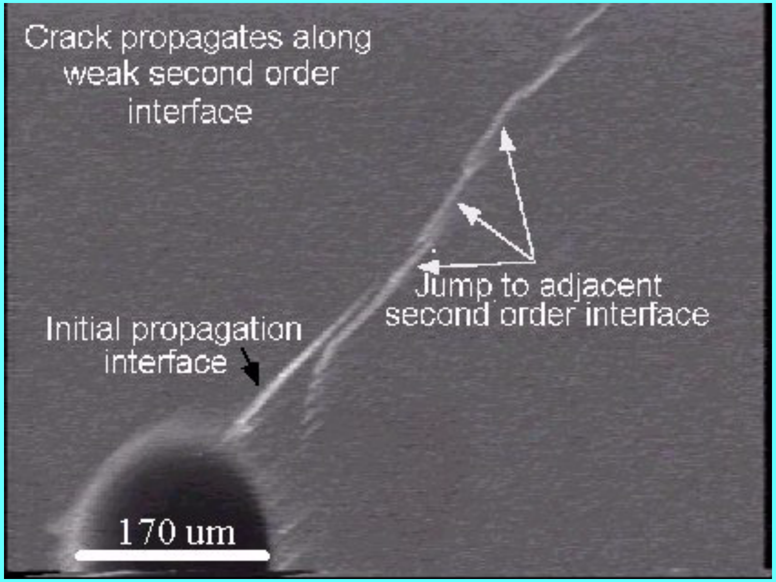
Crack propagates along
weak second order
interface
Jump to adjacent
second order interface
Initial propagation
interface
170 um

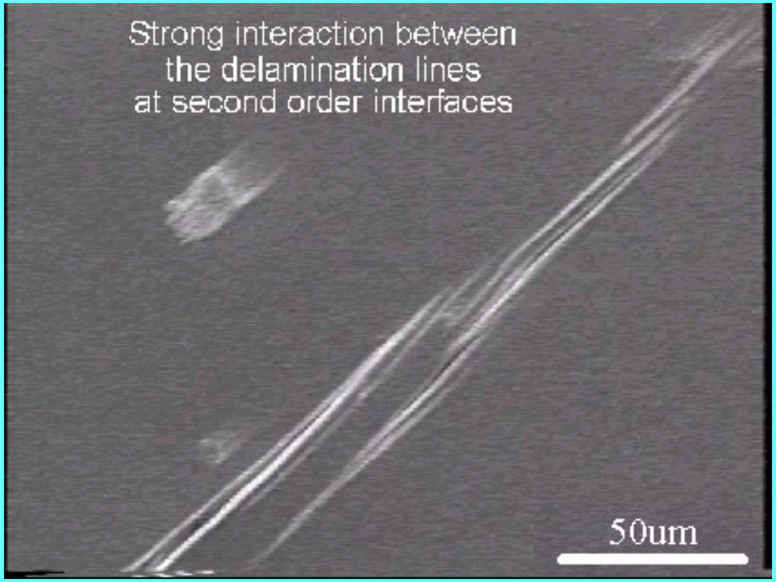
Strong interaction between
the delamination lines
at second order interfaces
50um

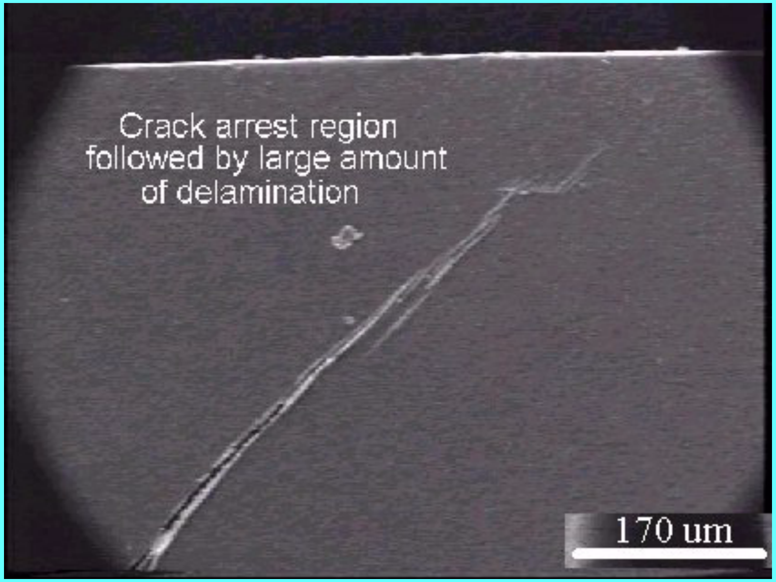
Crack arrest region
followed by large amount
of delamination
170 um

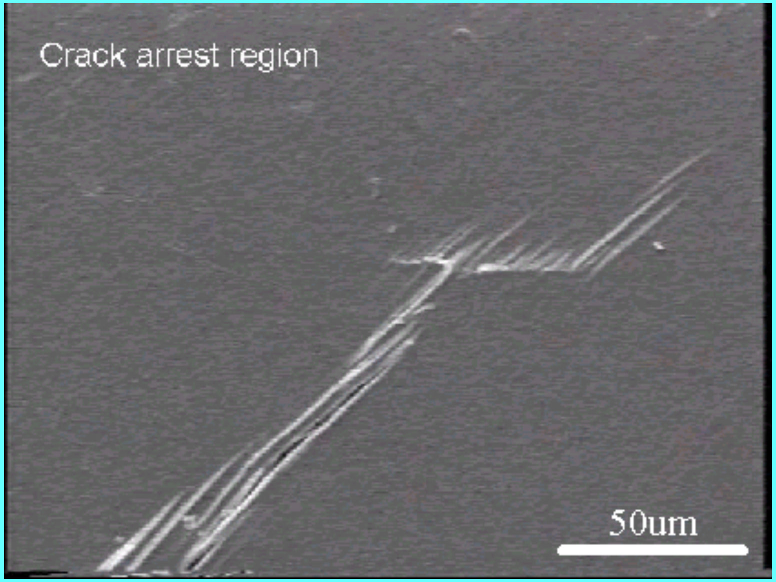
Crack arrest region
50um

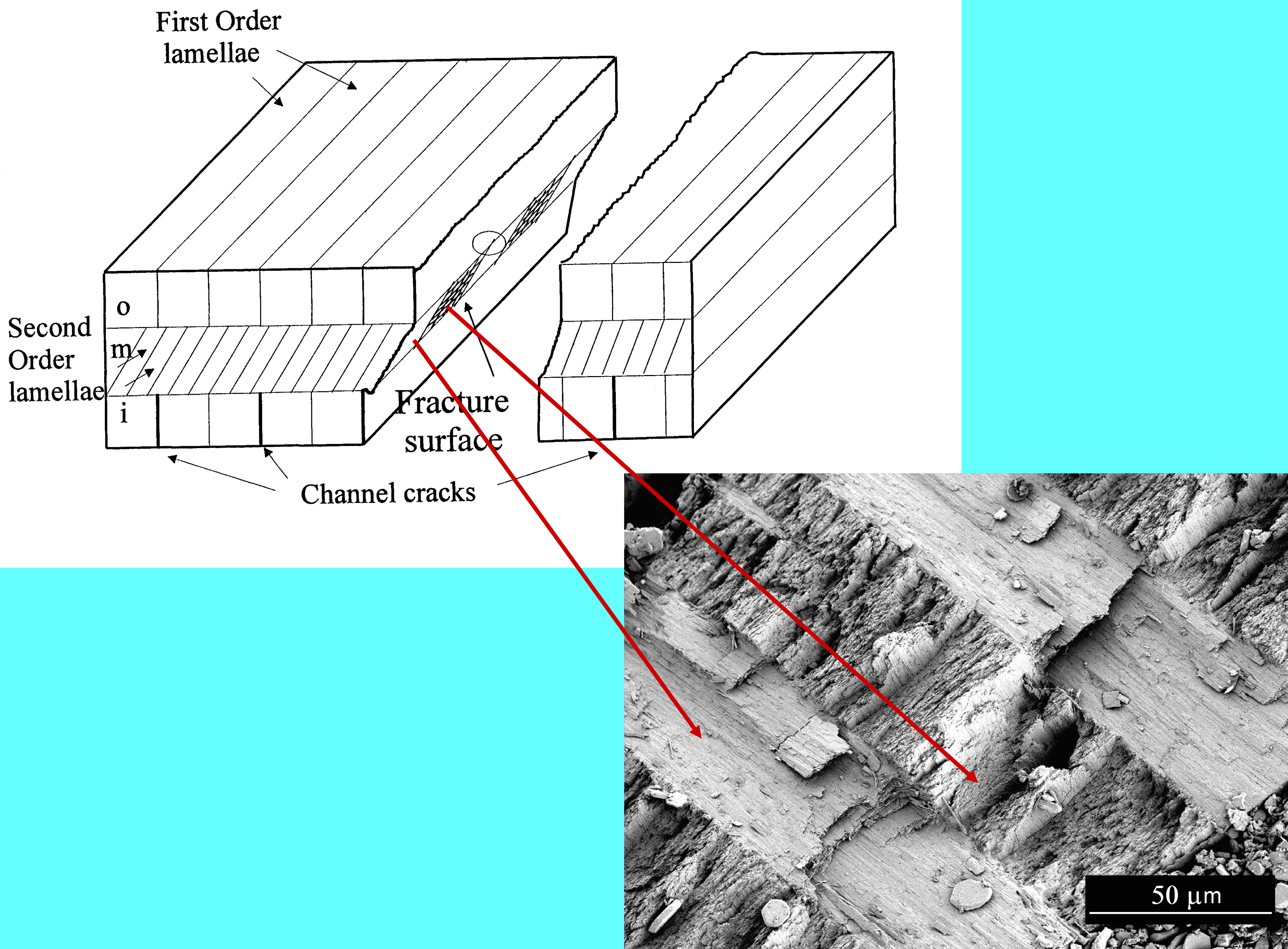
First Order
lamellae
Second
Order
lamellae
o
m
i
Fracture
surface
Channel cracks
50 μm

Multiple cracking of weak interface

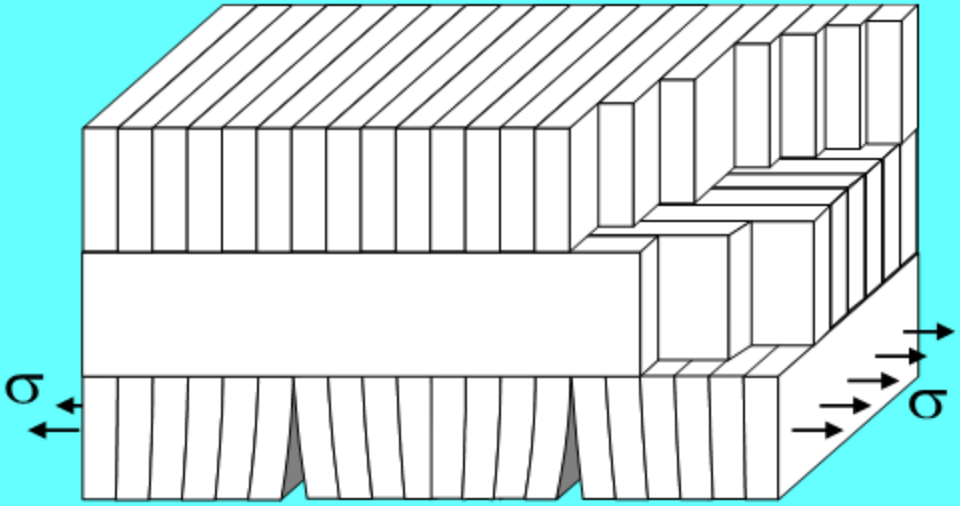

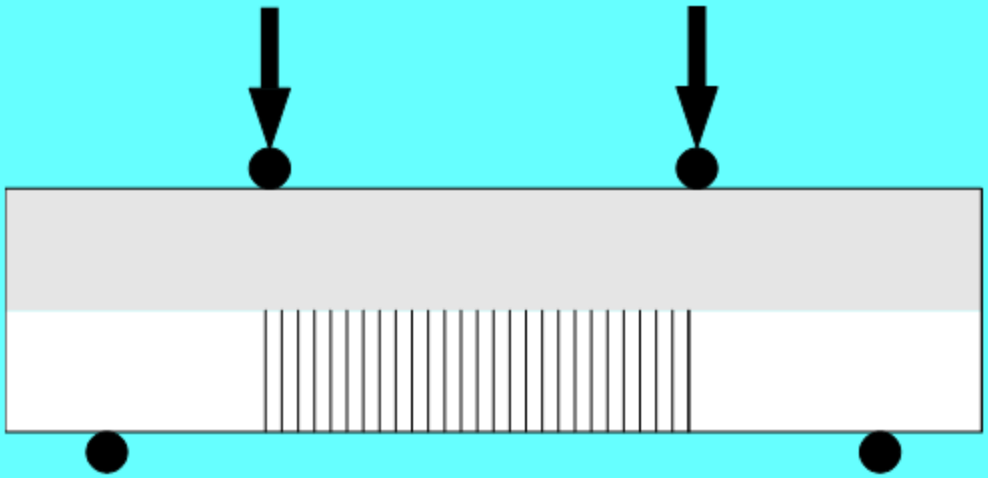

Cracking conditions

steady state growth
from large flaws

$$\left(\frac{\partial U_{total}}{\partial n}\right)_{\varepsilon} = 0$$

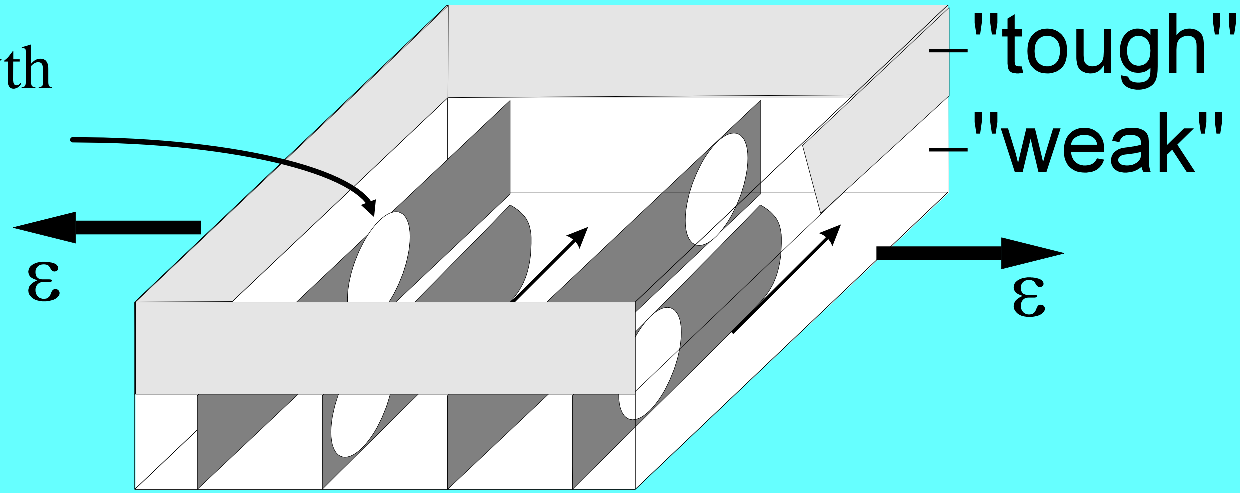

initiation of small flaws
by critical surface stress

$$\sigma_{surface}(\varepsilon) = \sigma_c$$

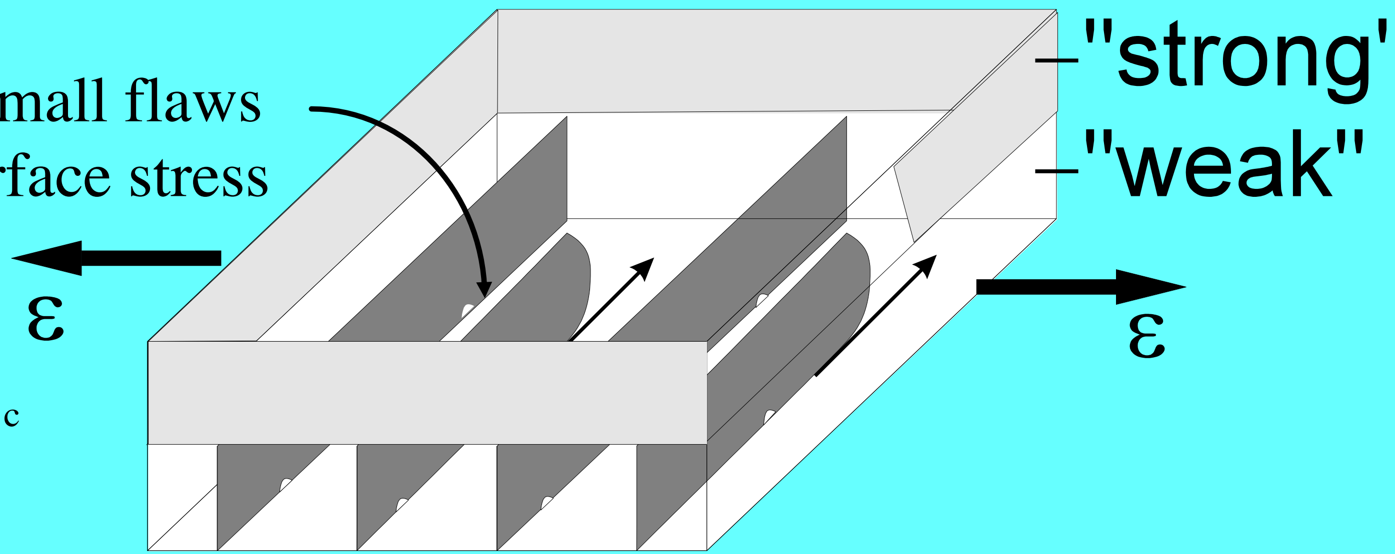

Basic idea (toughening)

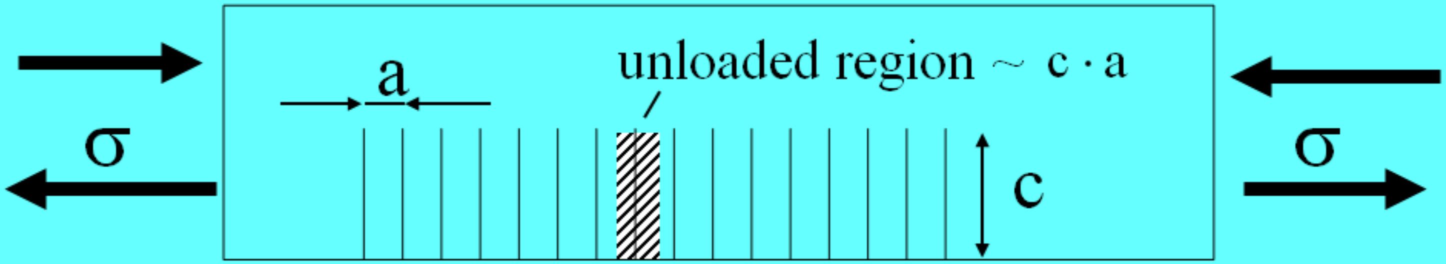

<u>Crack energy balance</u> :

strain energy → $c \cdot a \times \frac{\sigma^2}{E} \sim c \times \gamma$ ← surface energy

➡ Critical stress $\sigma_c \sim \left(\frac{\gamma E}{a}\right)^{1/2} \sim \frac{K_c}{a^{1/2}} >> \frac{K_c}{c^{1/2}}$

Shape function determination

$$f(n) = \frac{1}{2}\left(1 + \frac{1}{1 + 2\cdot|f'(0)|\cdot n}\right)$$

$$k(n) = \left(\frac{1 + pn}{1 + qn + sn^2}\right)^{1/2}$$

$$g(n) = \frac{1 - n/n_o}{1 + 8n - 5n^{3/2} + n^6}$$

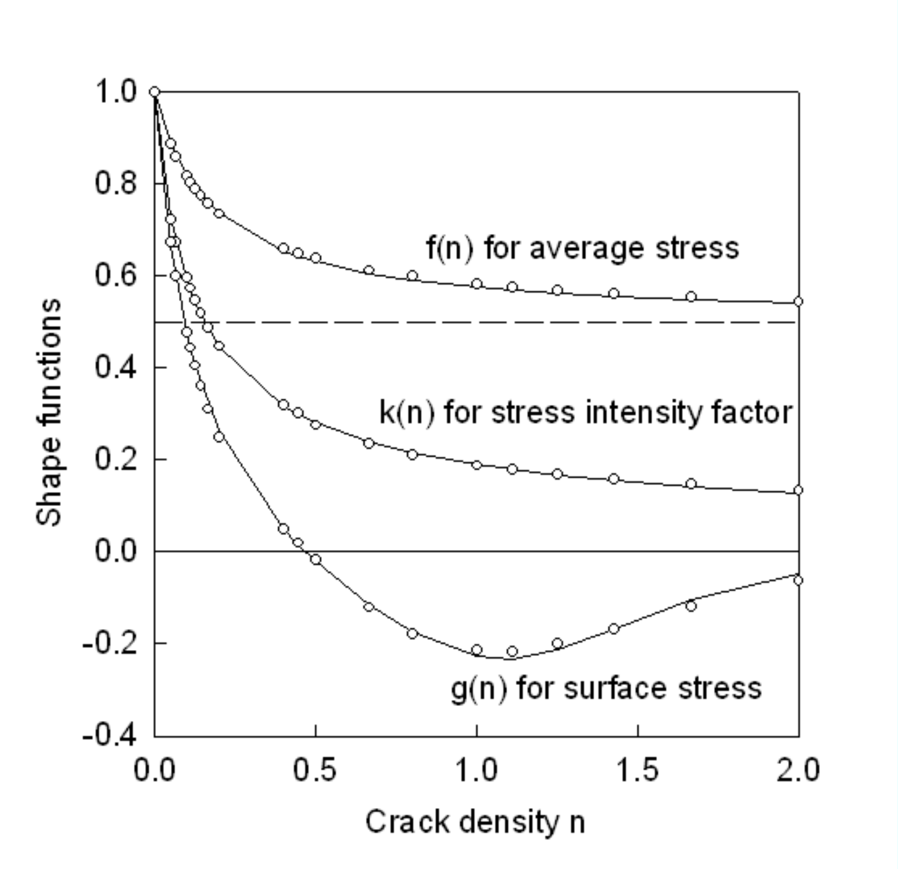

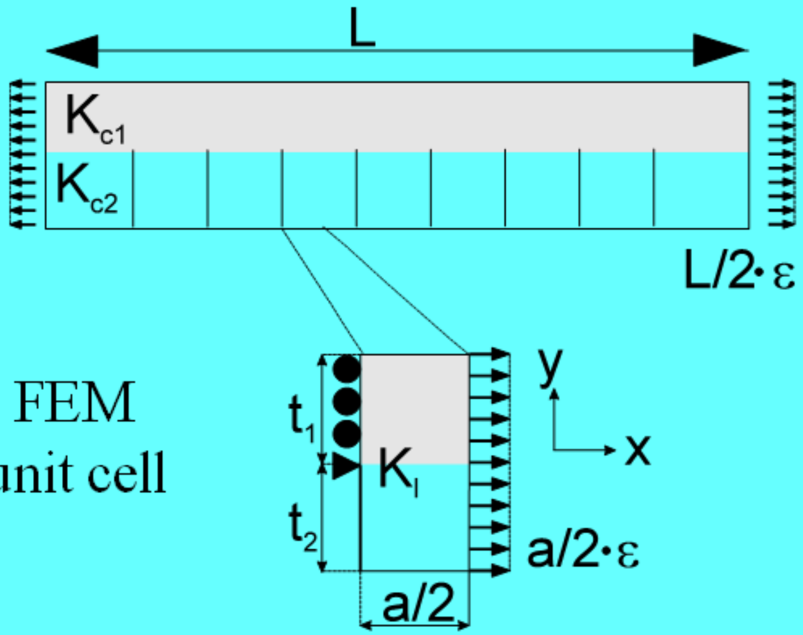

FEM
unit cell

Analysis

?	crack density evolution	$n=n(\varepsilon)$
?	stress-strain curve	$\sigma=\sigma(\varepsilon)$
?	failure stress and strain	$\sigma_{failure}$, $\varepsilon_{failure}$
?	work of fracture	$W_{fracture}$

Crack density at failure

Large flaws

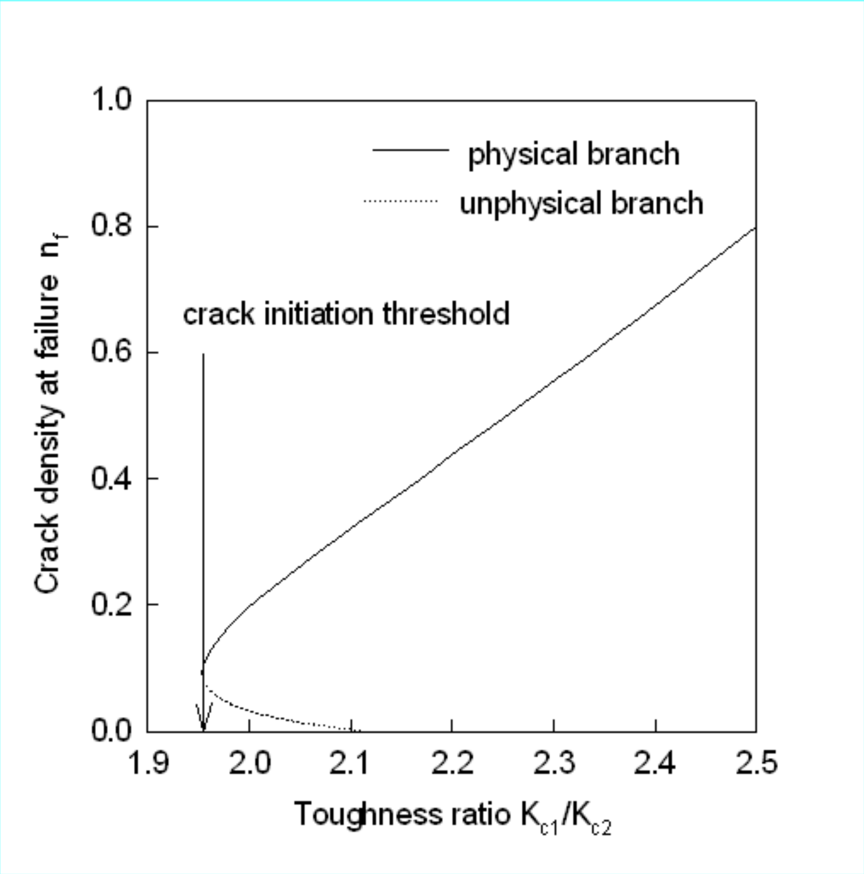

Small flaws

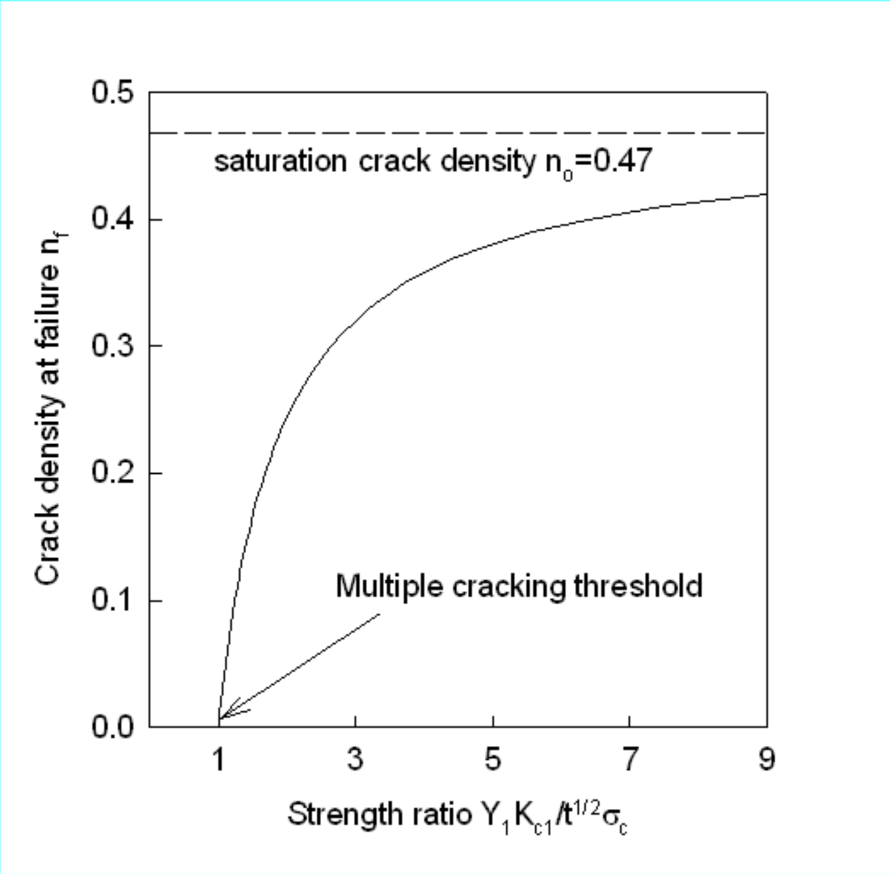

Stress and strain to failure

Large flaws

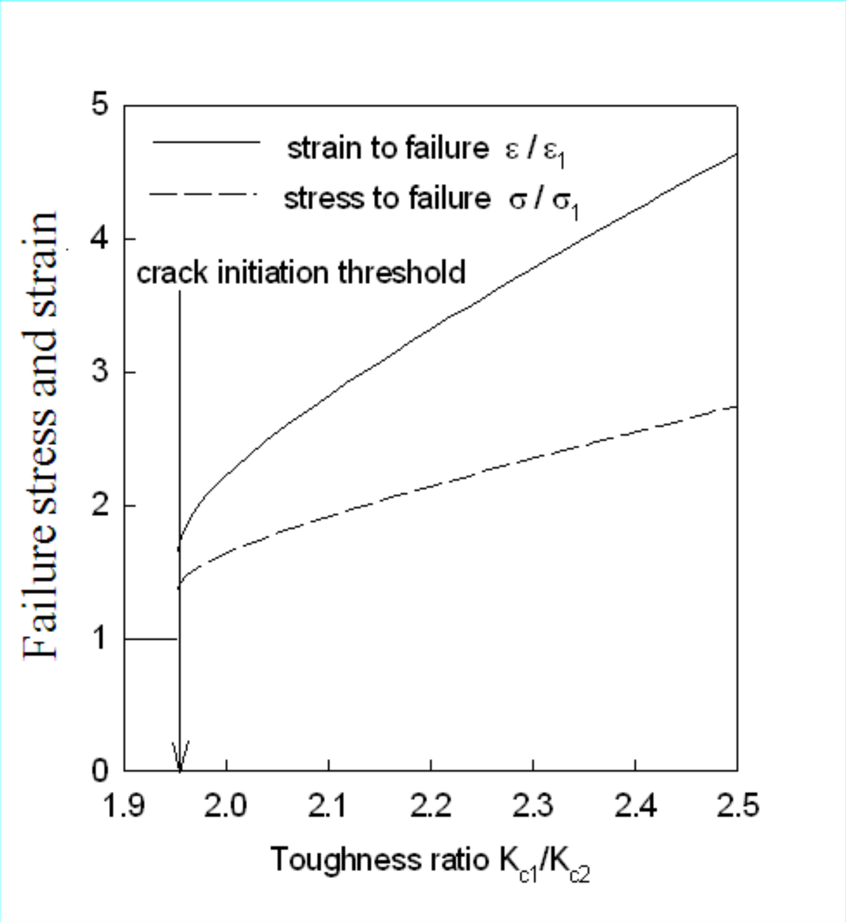

Small flaws

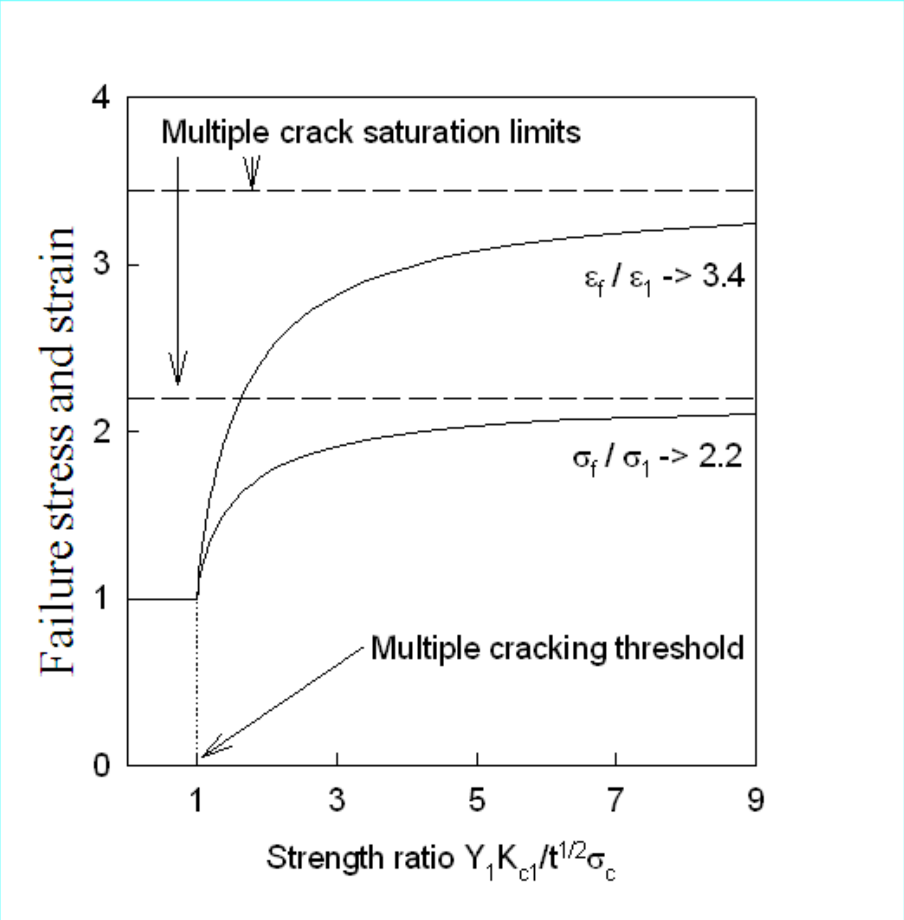

Work of fracture

Large flaws

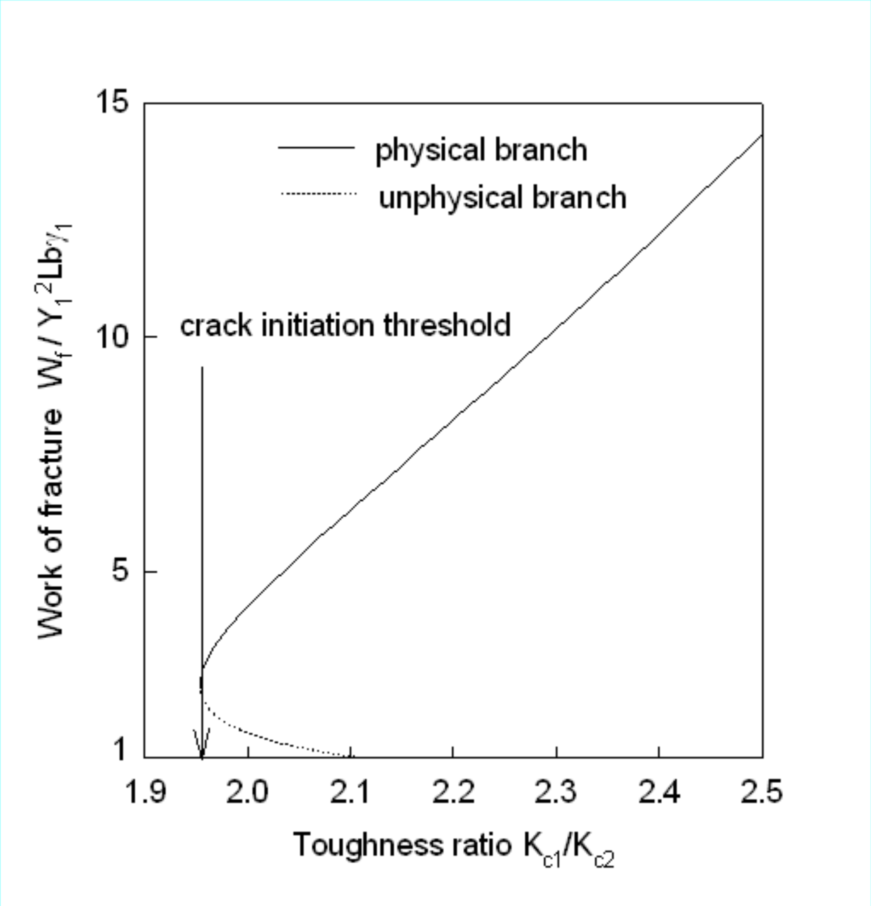

Small flaws

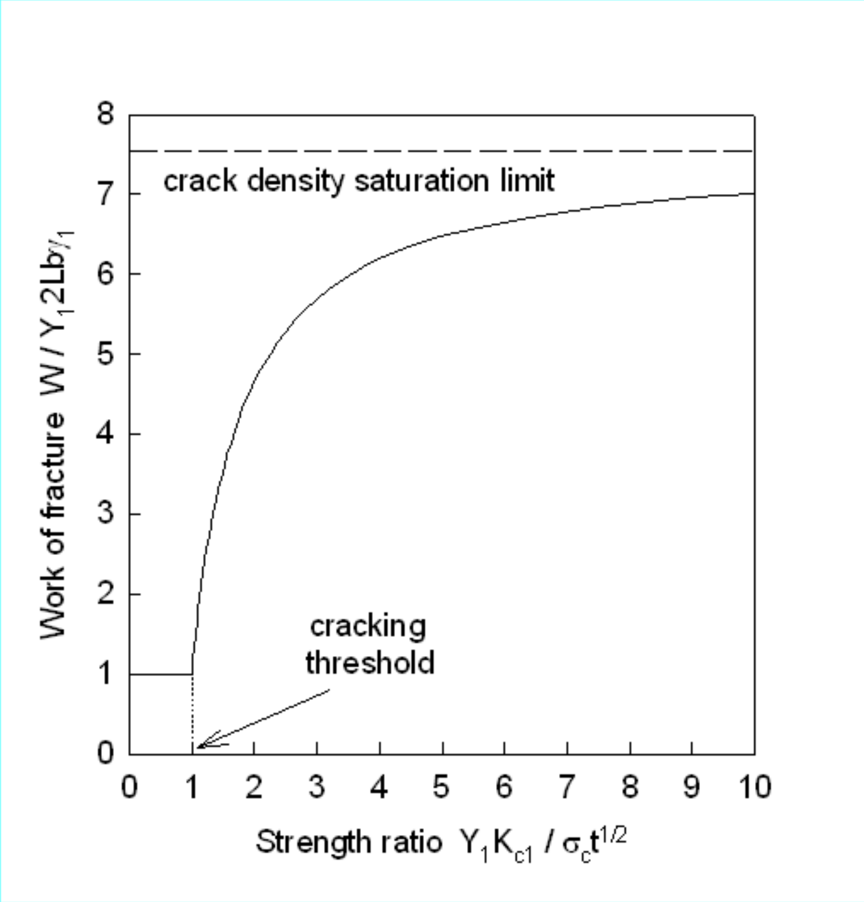

LARGE SCALE BRIDGING

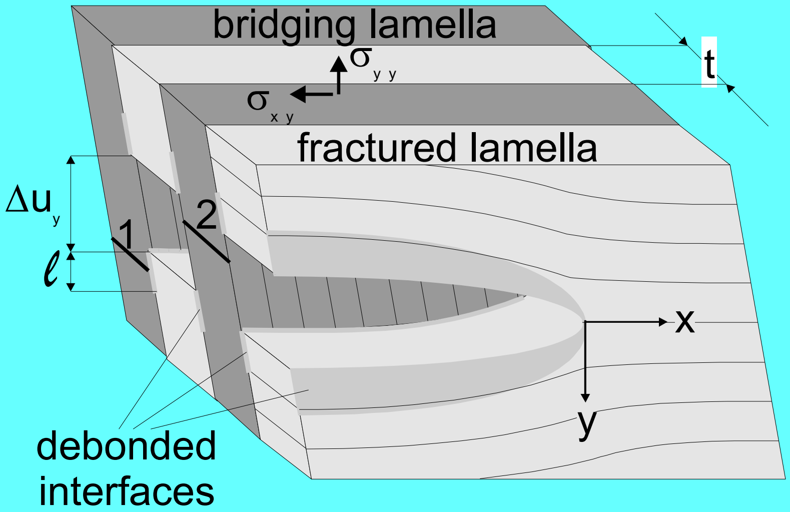

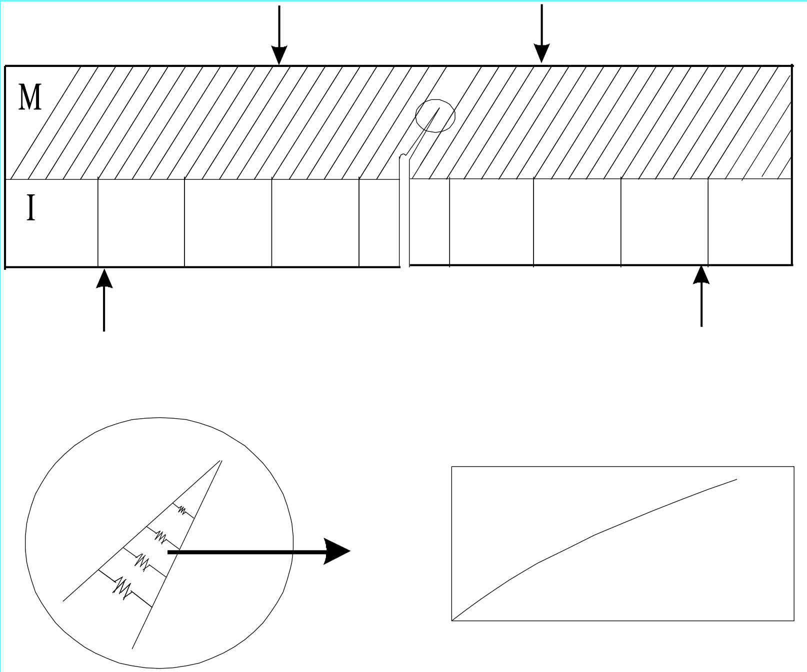

$K_{protein} = K_{far\text{-}field} - K_{bridging\ forces} = 0.6 MPa\text{-}m^{1/2}$

$p = \beta * u^{1/2}$: $\beta = 630\ N/mm^{5/2}$, $u_{crit} = 5\ \mu m$

$$J_b = \int_0^{u_{cr}} p(u)du = 150 N/m$$

$J_{aragonite} = (K^2/E)_{aragonite} = 0.63 N/m$

$J_{int} = 0.6^2/37 GPa = 9.7 N/m$

Work of fracture

Large flaws

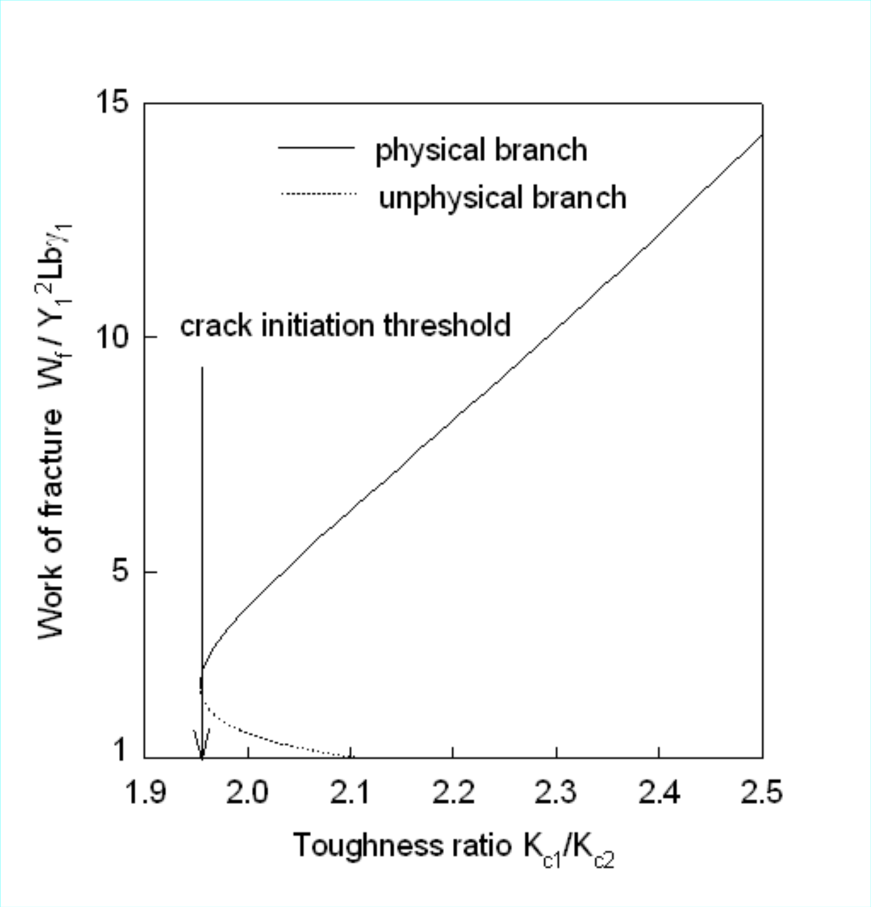

Small flaws

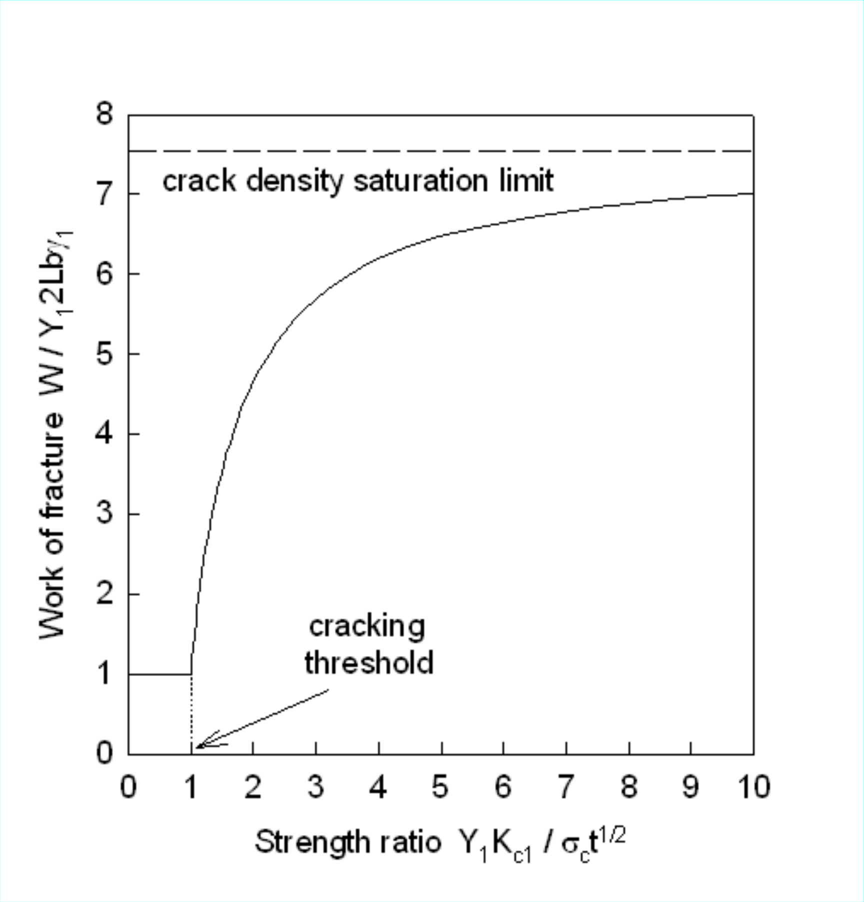

LARGE SCALE BRIDGING

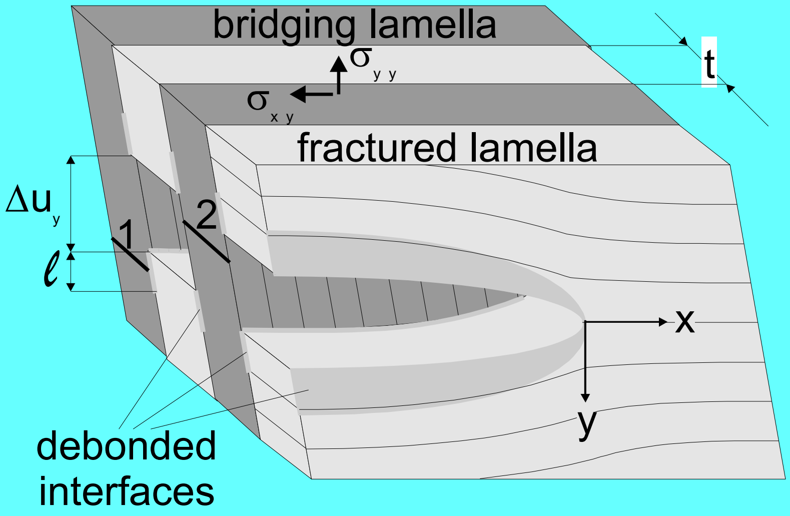

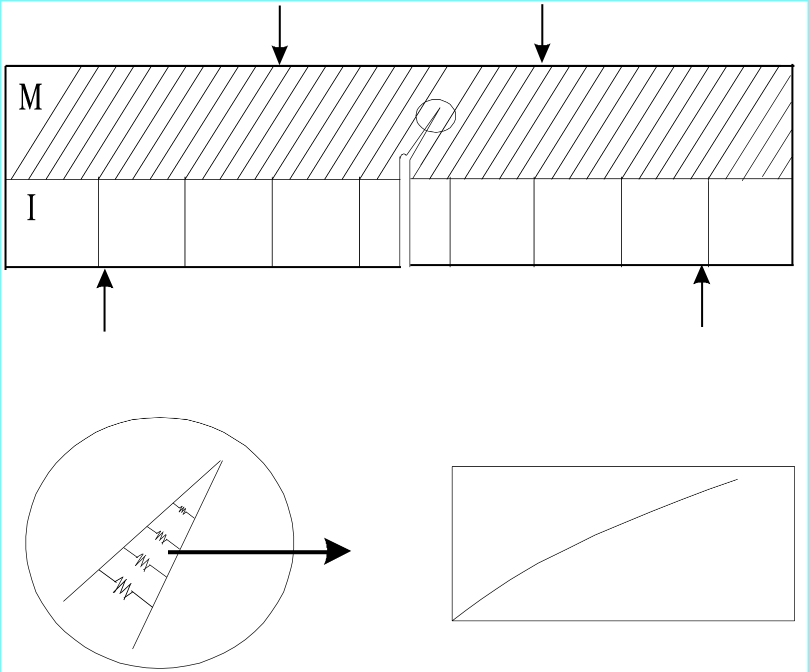

$K_{protein} = K_{far\text{-}field} - K_{bridging\ forces} = 0.6 MPa\text{-}m^{1/2}$

$p = \beta^* u^{1/2}$: $\beta = 630\ N/mm^{5/2}$, $u_{crit} = 5\ \mu m$

$$J_b = \int_0^{u_{cr}} p(u)du = 150 N/m$$

$J_{aragonite} = (K^2/E)_{aragonite} = 0.63 N/m$

$J_{int} = 0.6^2/37 GPa = 9.7 N/m$

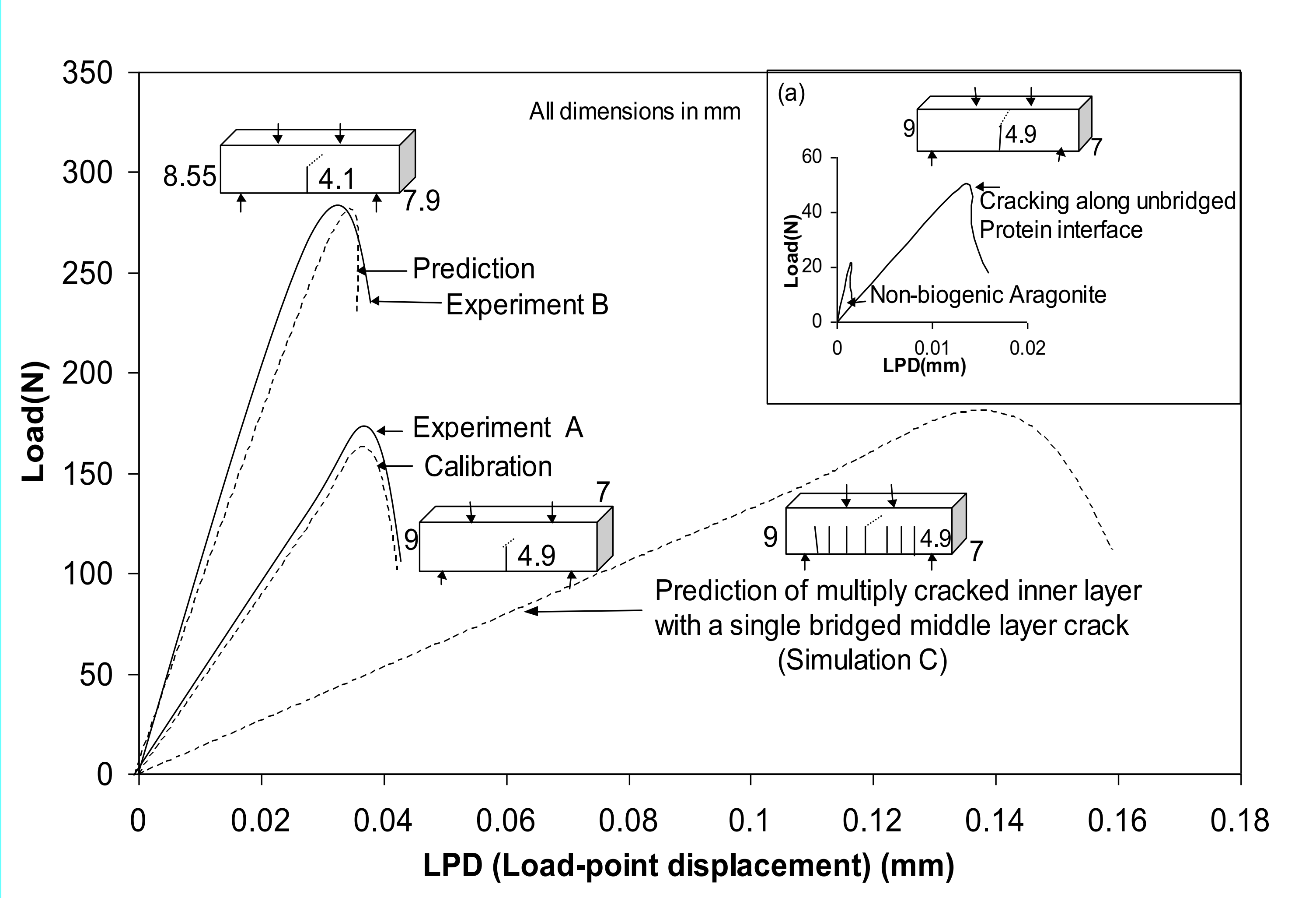

WORK OF FRACTURE (E-3J)

Aragonite	Protein	Notched A	Multiply Cracked
0.07	0.4	5.8	23

-120ºC

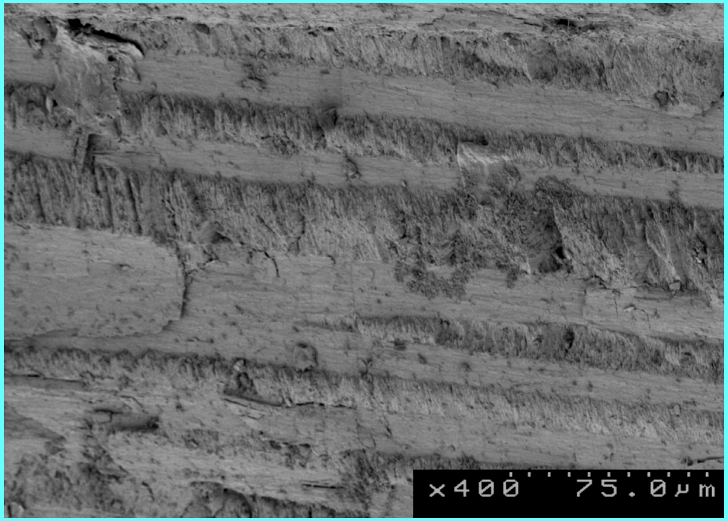

200ºC

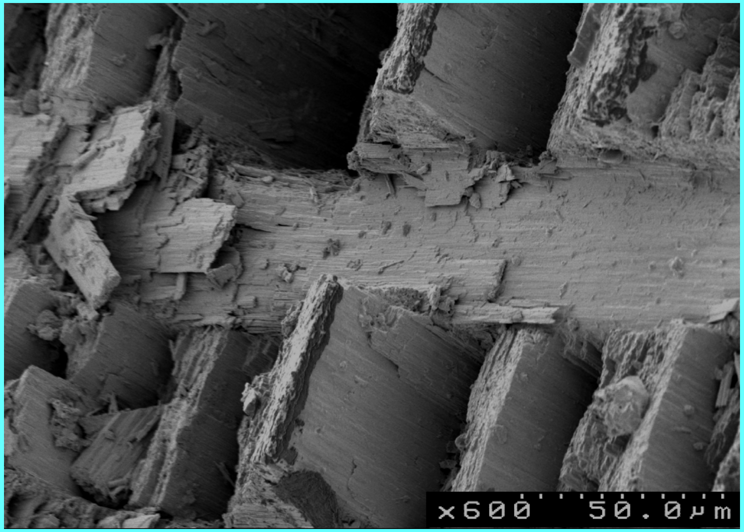

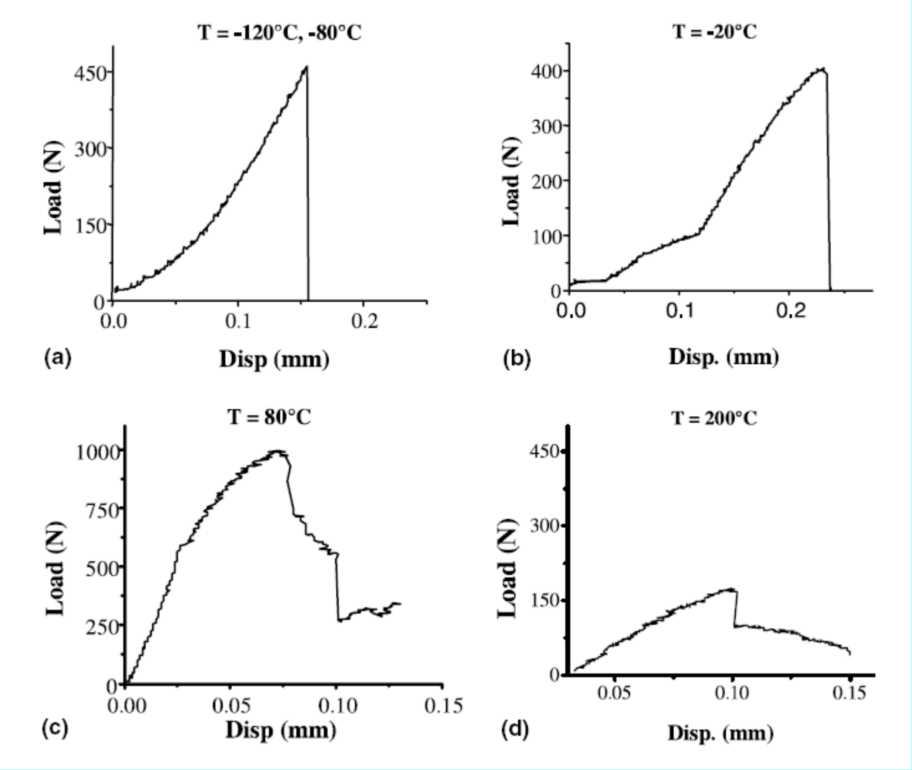

Role of the binder

Modular Elongation Mechanism

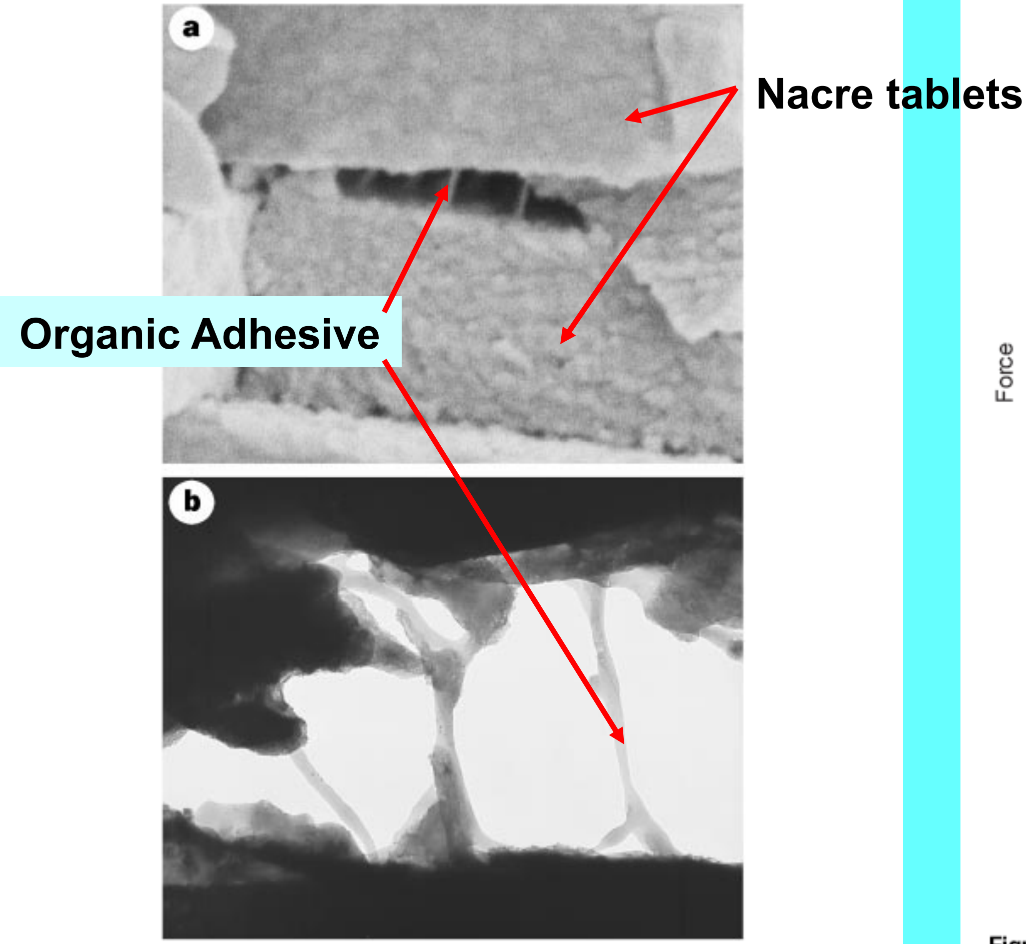

Figure 1 Scanning and transmission electron micrographs of a freshly cleaved abalone shell, showing adhesive ligaments formed between nacre tablets. **a**, Scanning electron micrograph of a freshly cleaved abalone shell showing adhesive ligaments formed between consecutive abalone nacre tablets on exertion of mechanical stress. The tablets are ~400 nm thick. **b**, Transmission electron micrograph of another cleaved abalone shell, showing the adhesive ligaments between nacre tablets. The space between the tablets is ~600 nm. Thus the ligaments can lengthen to many times the original spacing between the tablets, which is of the order of 30 nm.

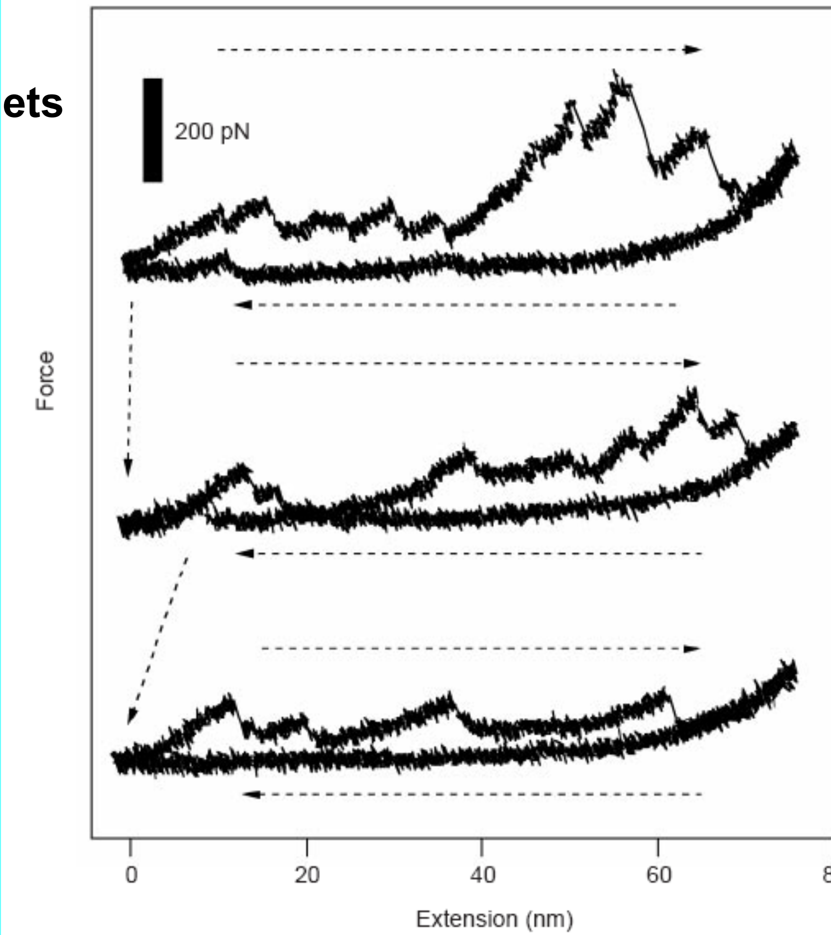

Figure 2 Consecutive force–extension curves, obtained using an atomic force microscope, from pulling on a freshly cleaved abalone nacre surface. Rupture events, with a sawtooth appearance, are visible in each of the curves. The surface was not touched between pulls, strong evidence that some refolding took place, possibly of domains in lustrin A. The approach and retract curves show hysteresis, indicating that the rupture events dissipate energy.

B.L. Smith et al., Nature, 1999

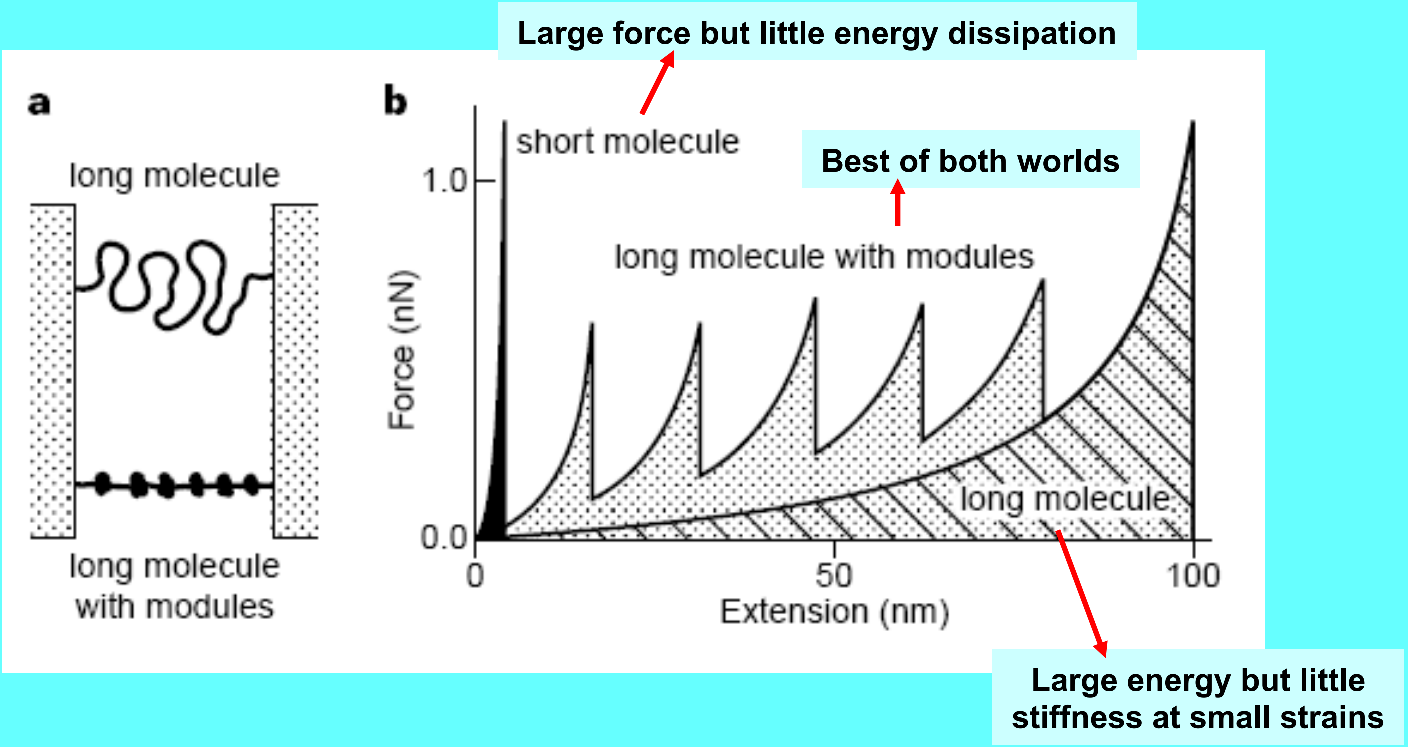

Large force but little energy dissipation
Best of both worlds
Large energy but little stiffness at small strains
a
long molecule
long molecule
with modules
b
short molecule
long molecule with modules
long molecule
1.0
0.0
Force (nN)
0
50
100
Extension (nm)

Schematic Drawing of Conch Shell

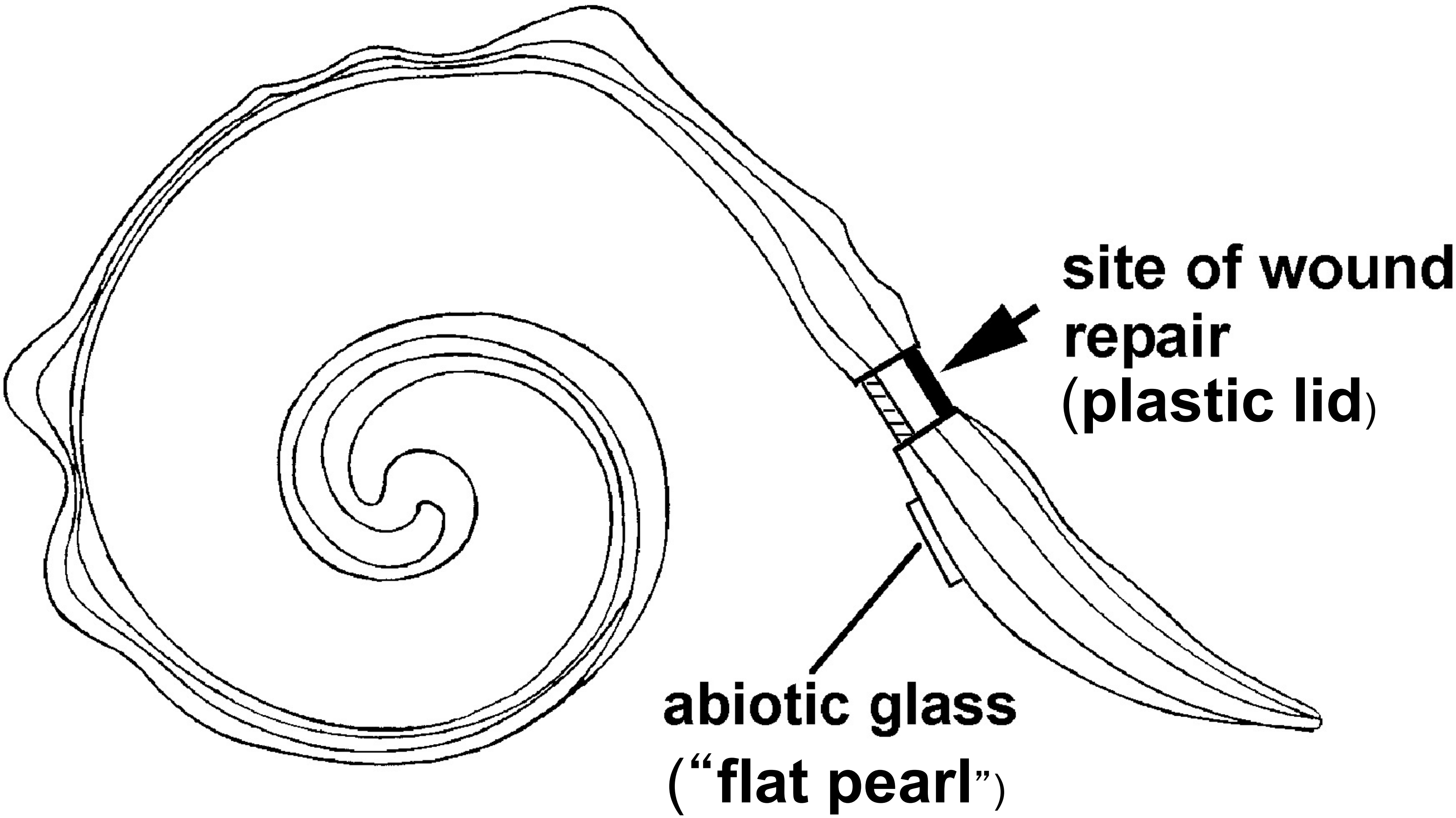

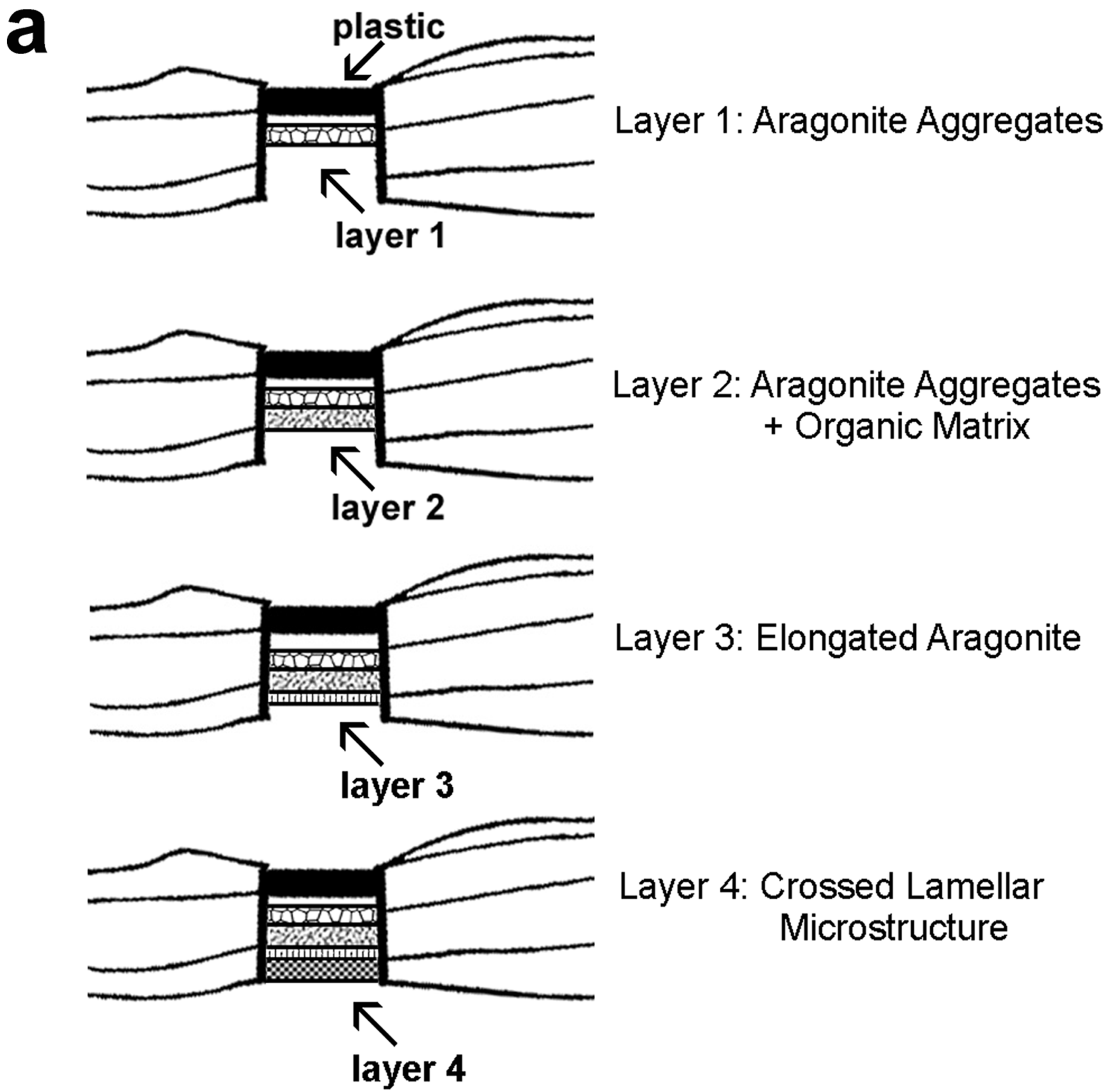
a
plastic
layer 1
Layer 1: Aragonite Aggregates
layer 2
Layer 2: Aragonite Aggregates
+ Organic Matrix
layer 3
Layer 3: Elongated Aragonite
layer 4
Layer 4: Crossed Lamellar
Microstructure

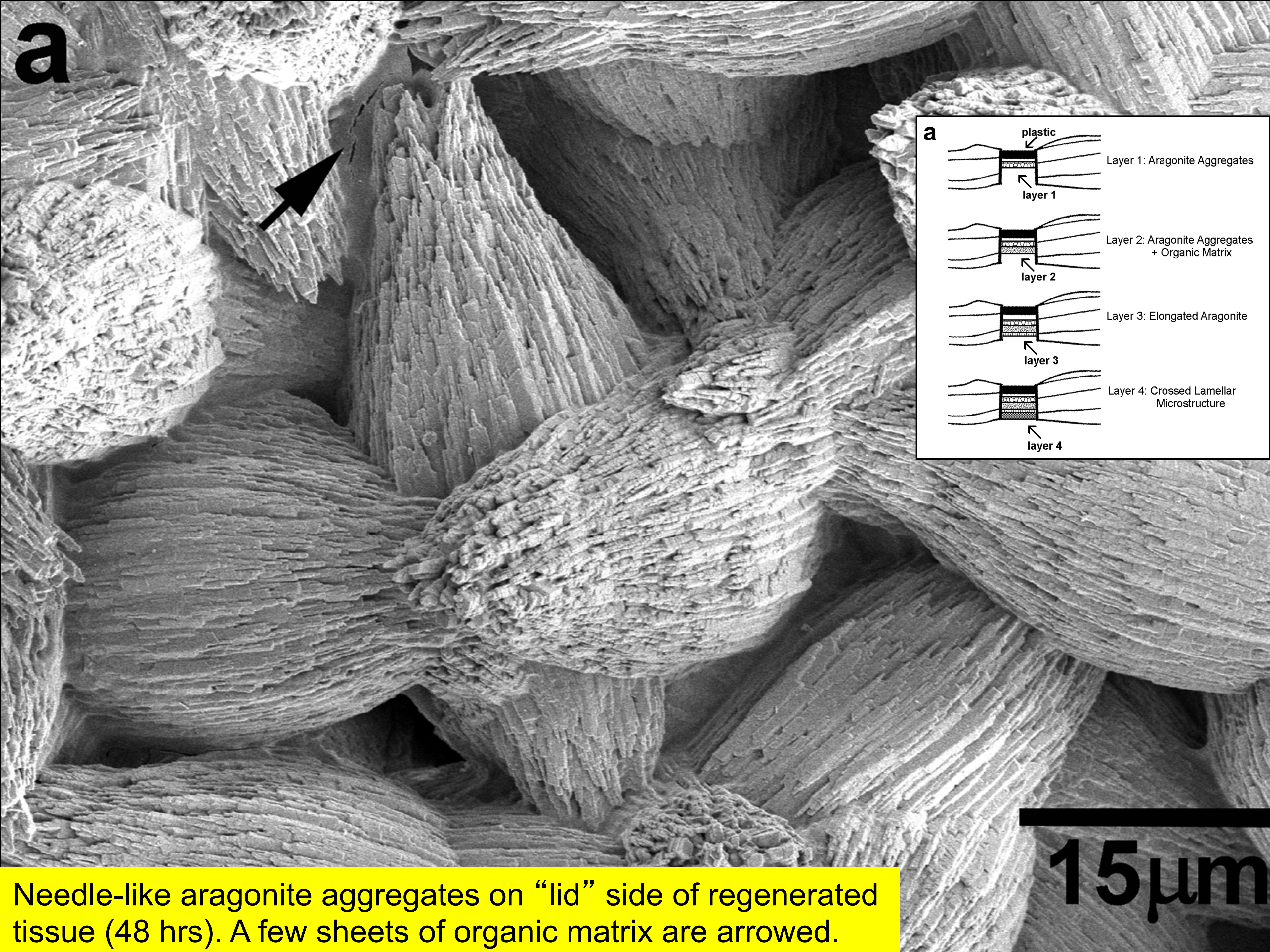

Needle-like aragonite aggregates on “lid” side of regenerated tissue (48 hrs). A few sheets of organic matrix are arrowed.

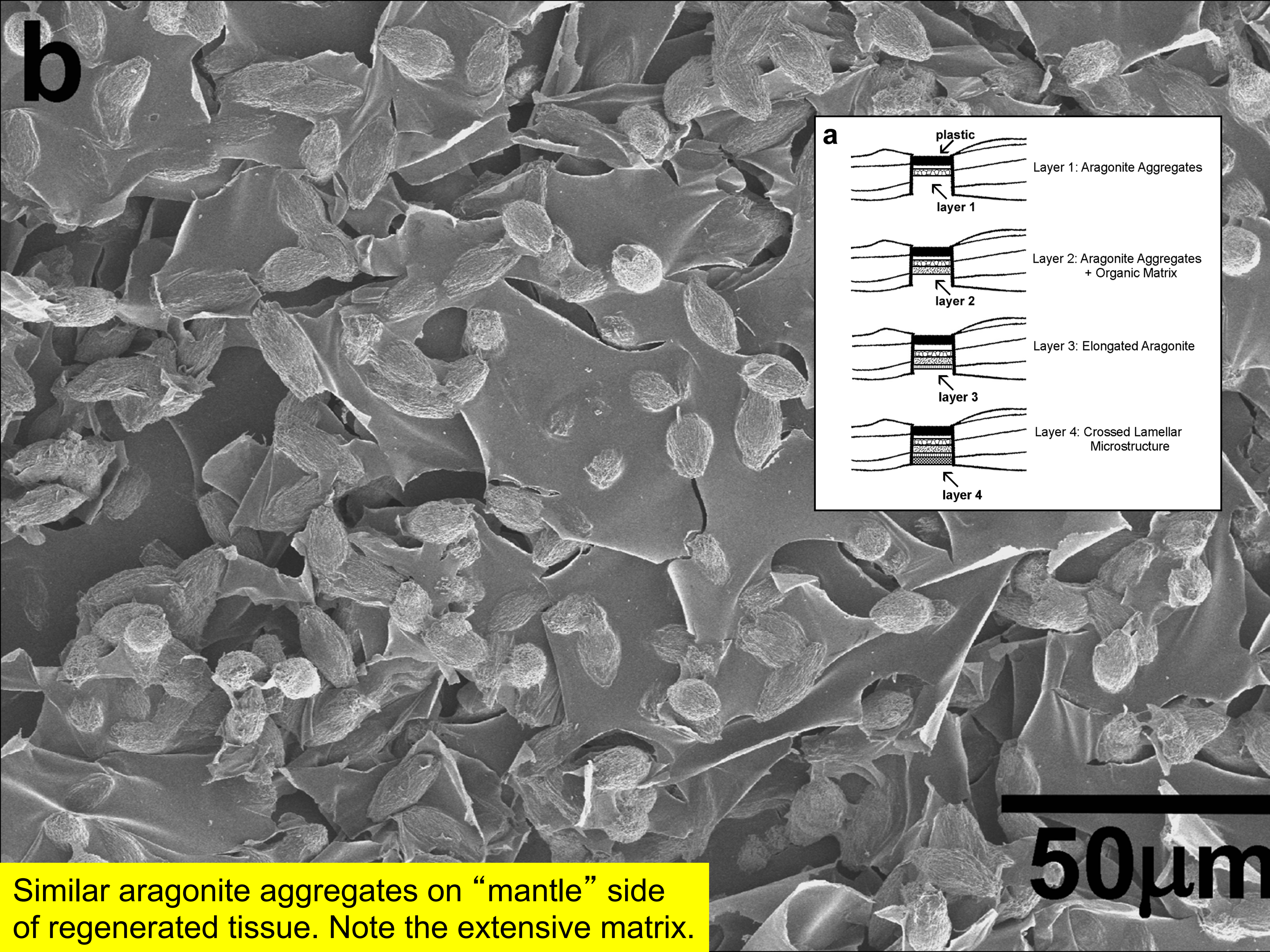

Similar aragonite aggregates on “mantle” side of regenerated tissue. Note the extensive matrix.

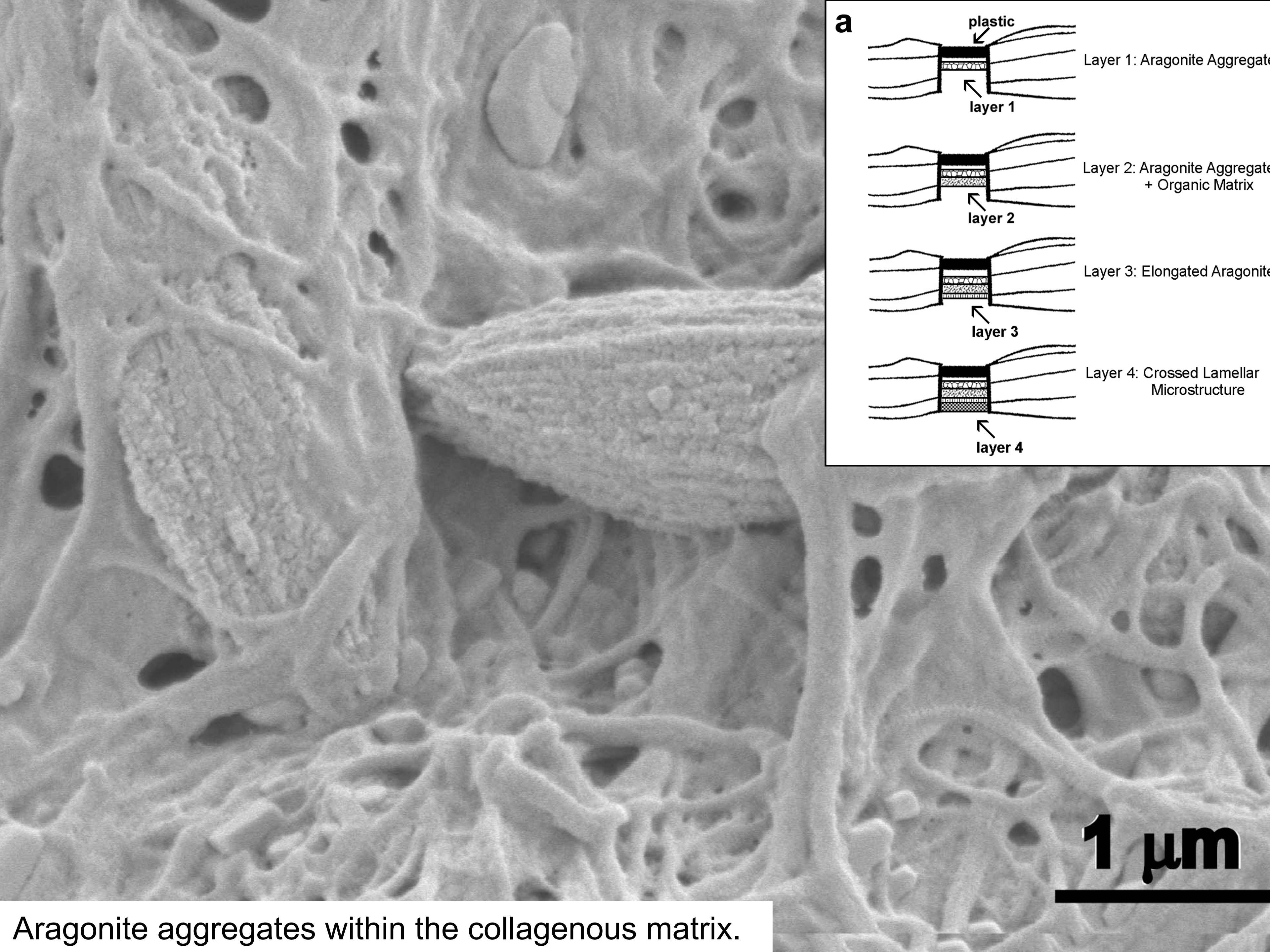

Aragonite aggregates within the collagenous matrix.

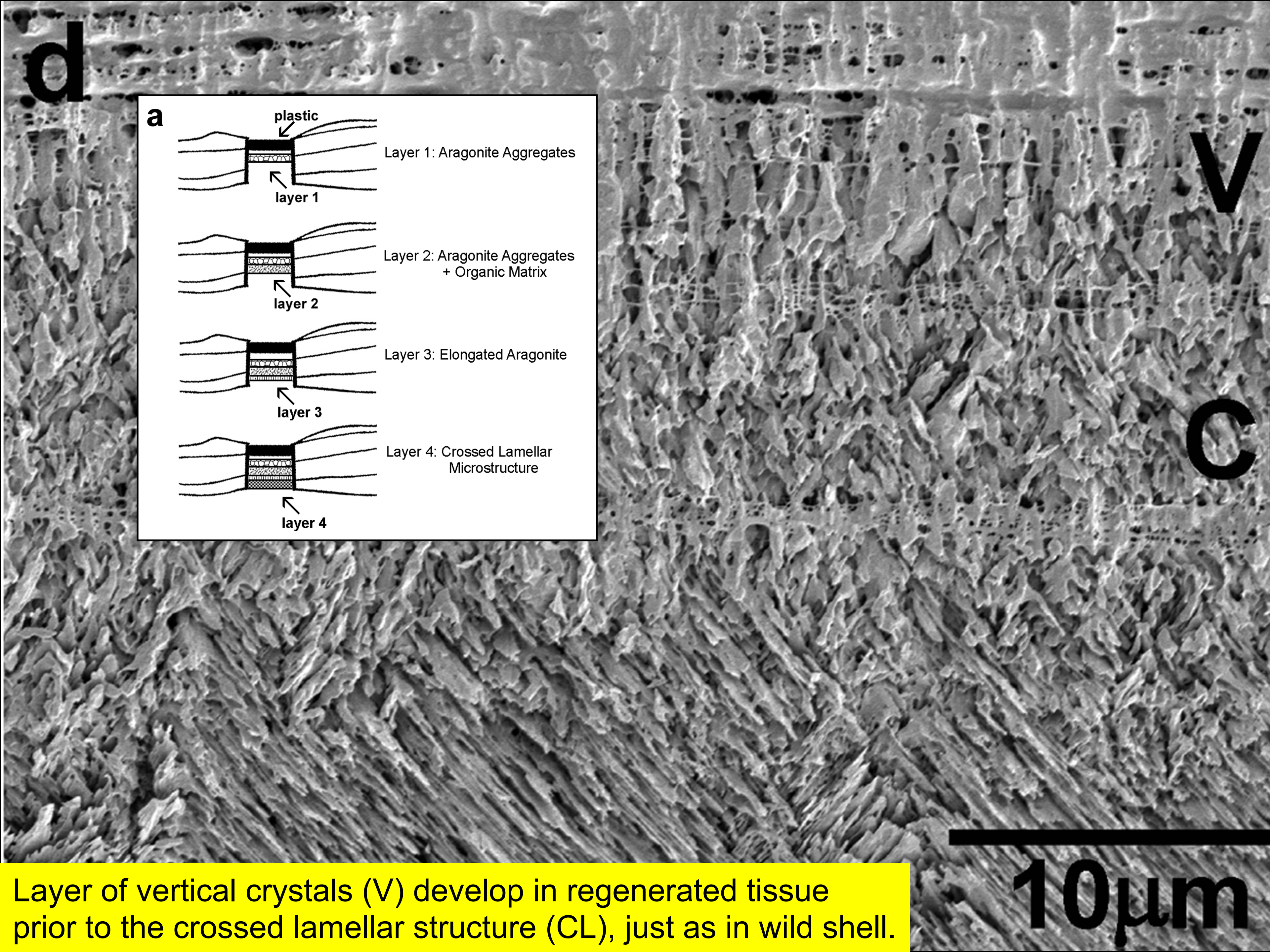

Layer of vertical crystals (V) develop in regenerated tissue prior to the crossed lamellar structure (CL), just as in wild shell.

BIOINSPIRED COMPOSITE STRUCTURES

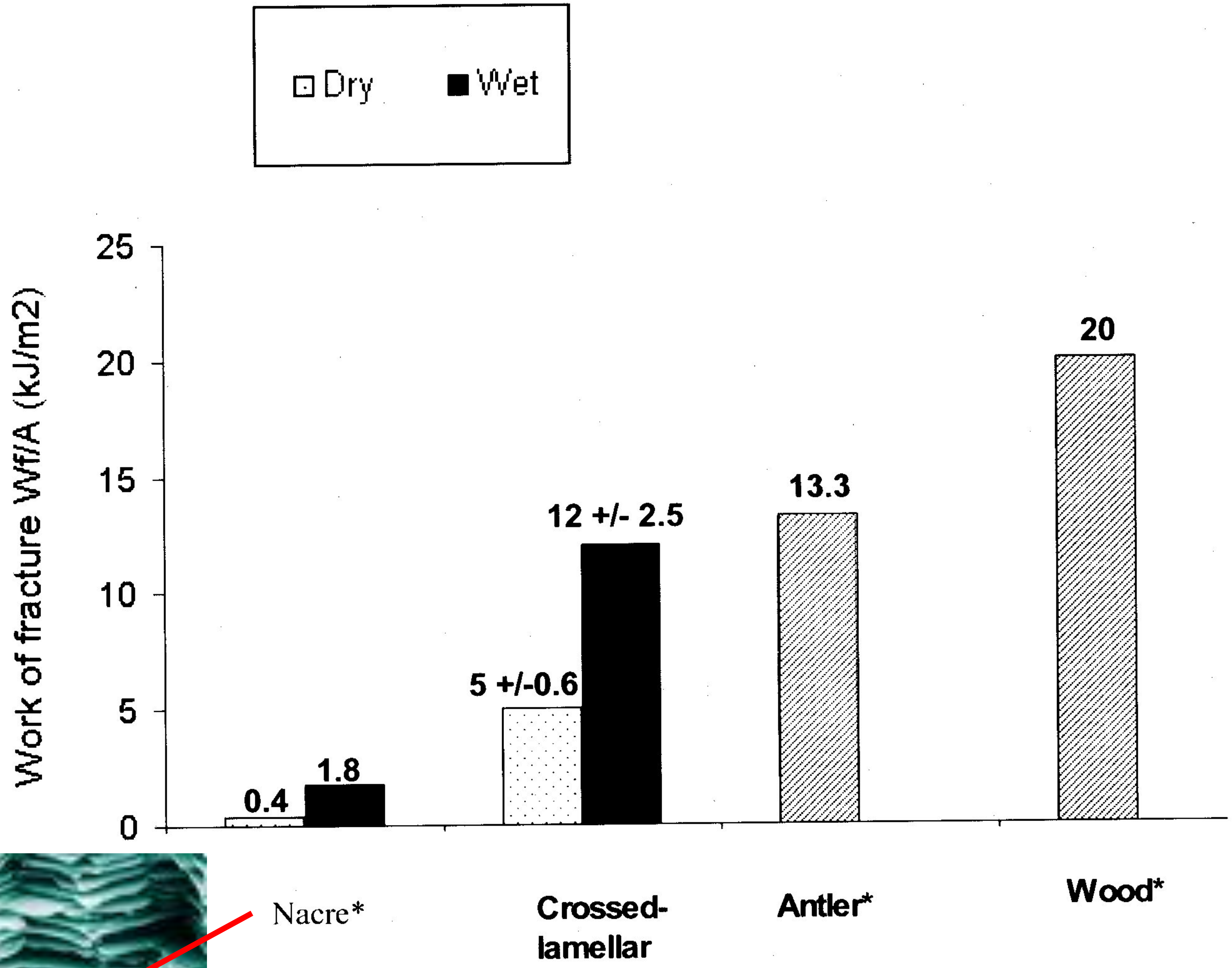

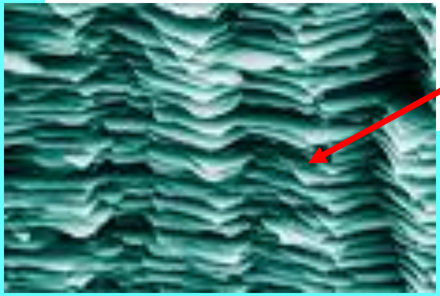

A.A.Jackson, J.F.V. Vincent and R.M. Turner (1990)
J. Mat. Sci. 25, p3137

Bioinspired Fabrication of Composites: Synthetic Nacre

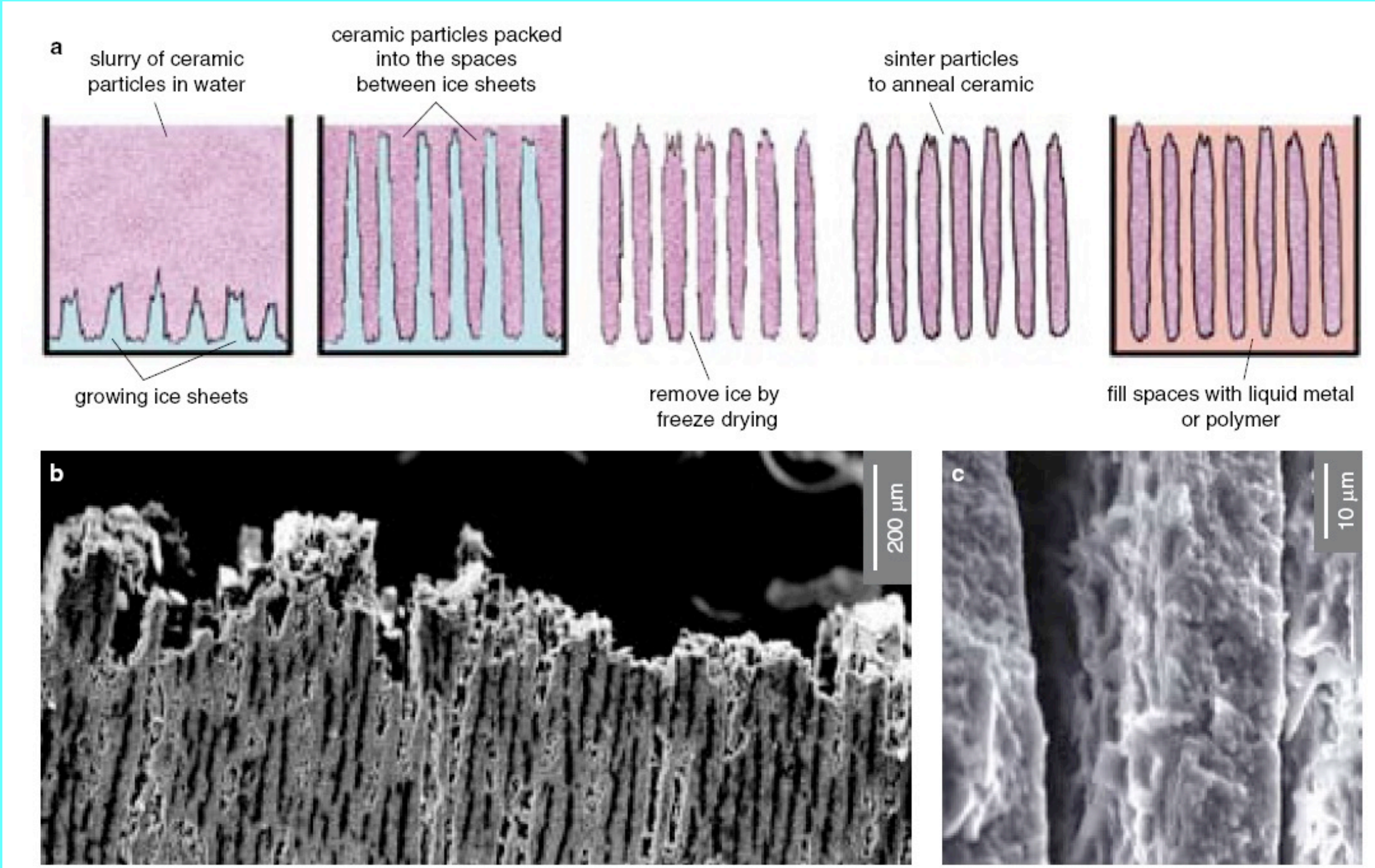

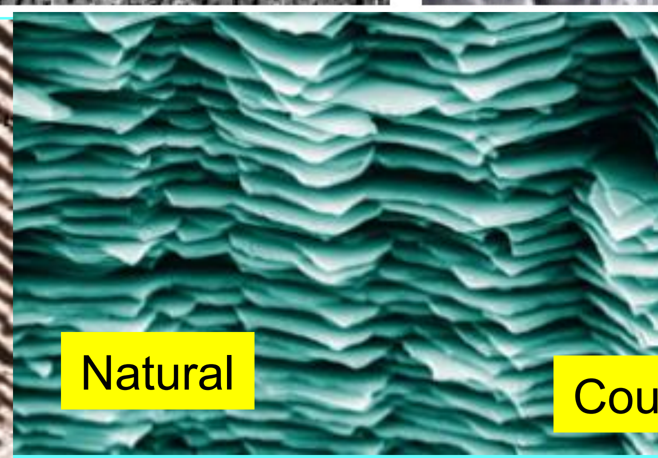

Courtesy of A. Tomasia

3-D Printing

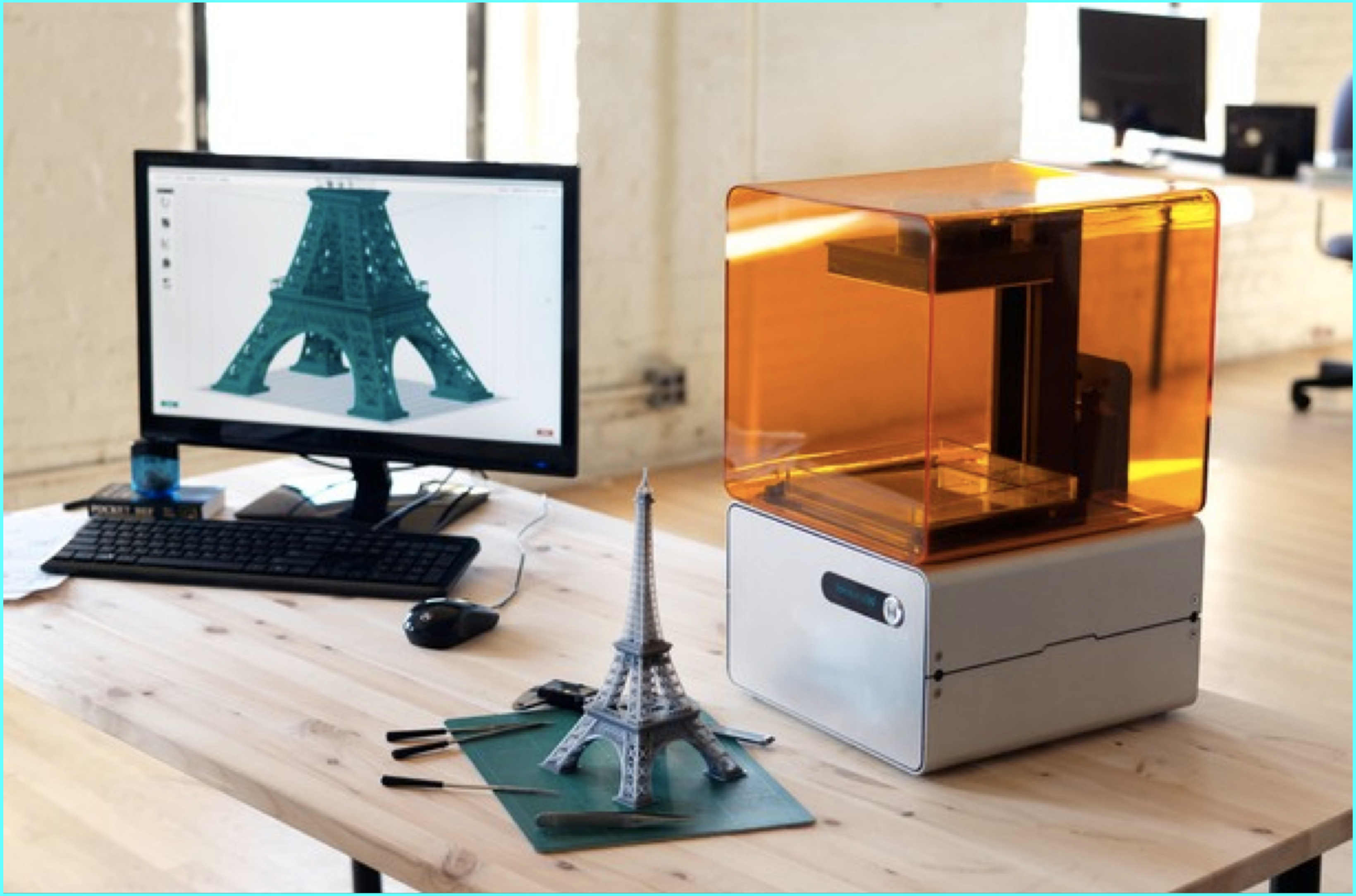

Bioinspired Self-Healing

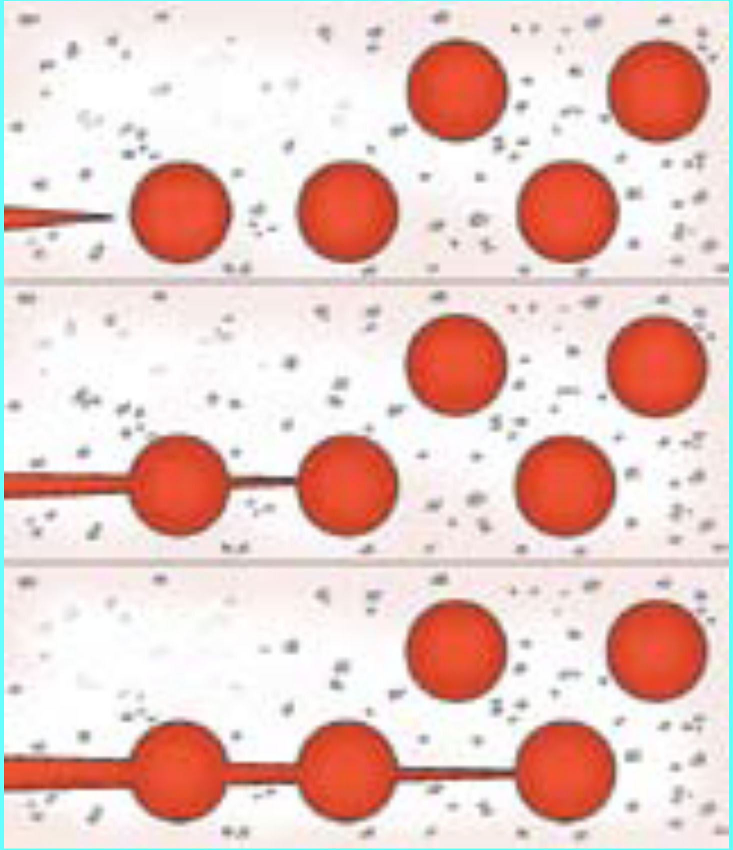

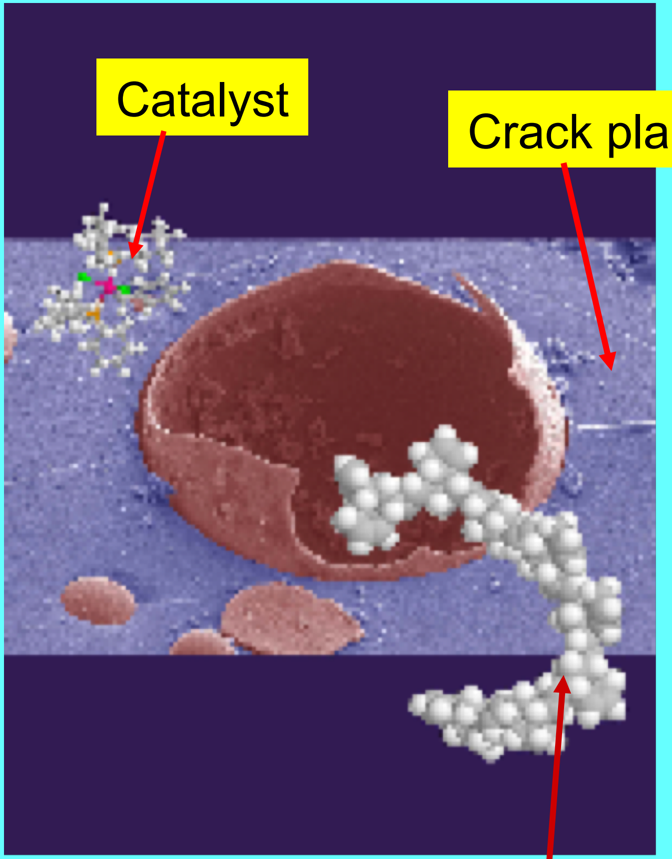

Courtesy of Nancy Sottos
University of Illinois

In the future the healing
materials will be delivered after damage is sensed.

Vascular Systems

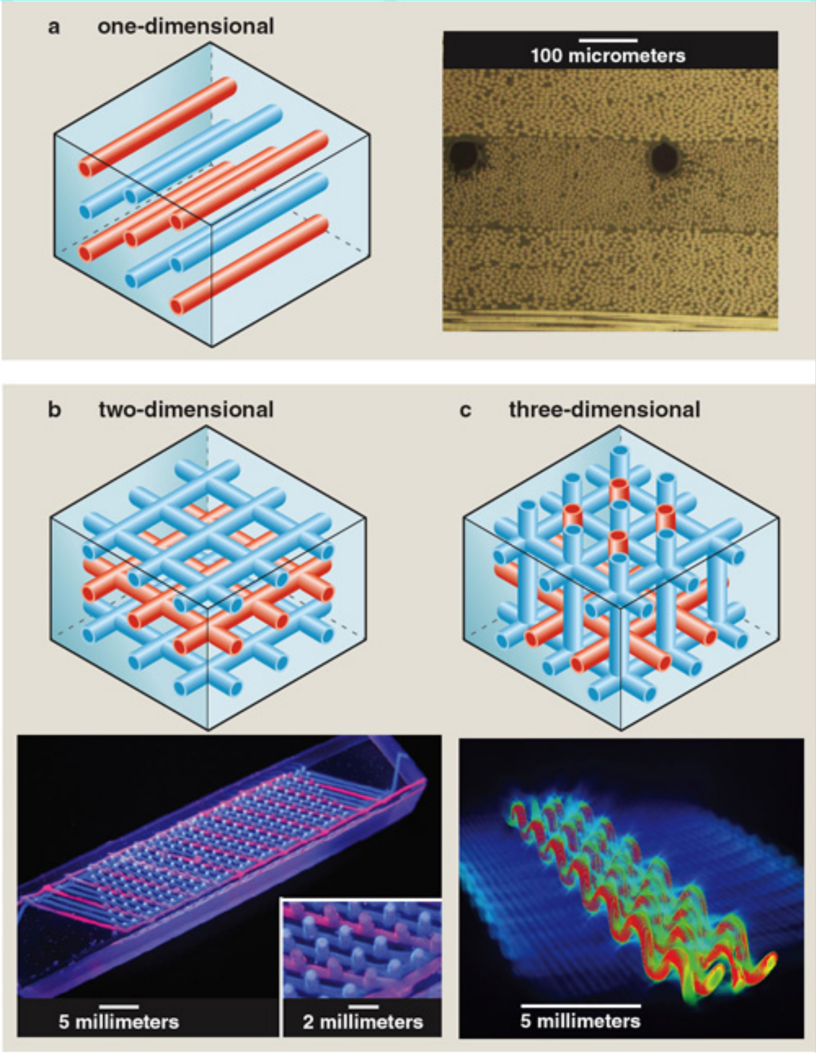

Self-Healing Concrete

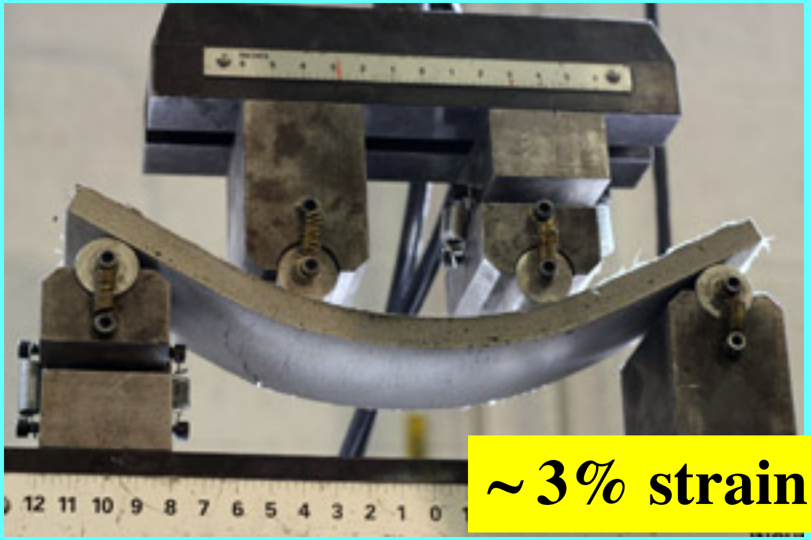

~3% strain

Reinforce such that crack widths are limited to 50 microns. Then the cement grains that have not reacted during original curing will react with added water and air to heal the cracks.

Victori Li's Group at U. Michigan

Other approaches considered around the world

Biomineralization using "*Extremophiles*":

Incorporate calcium carbonate-producing bacteria in the concrete mix. Micro-organisms showing promise include *B. Pasteurii*.

Mondal, Struble and Liu, University of Illinois

Jonkers, TU Delft

Others